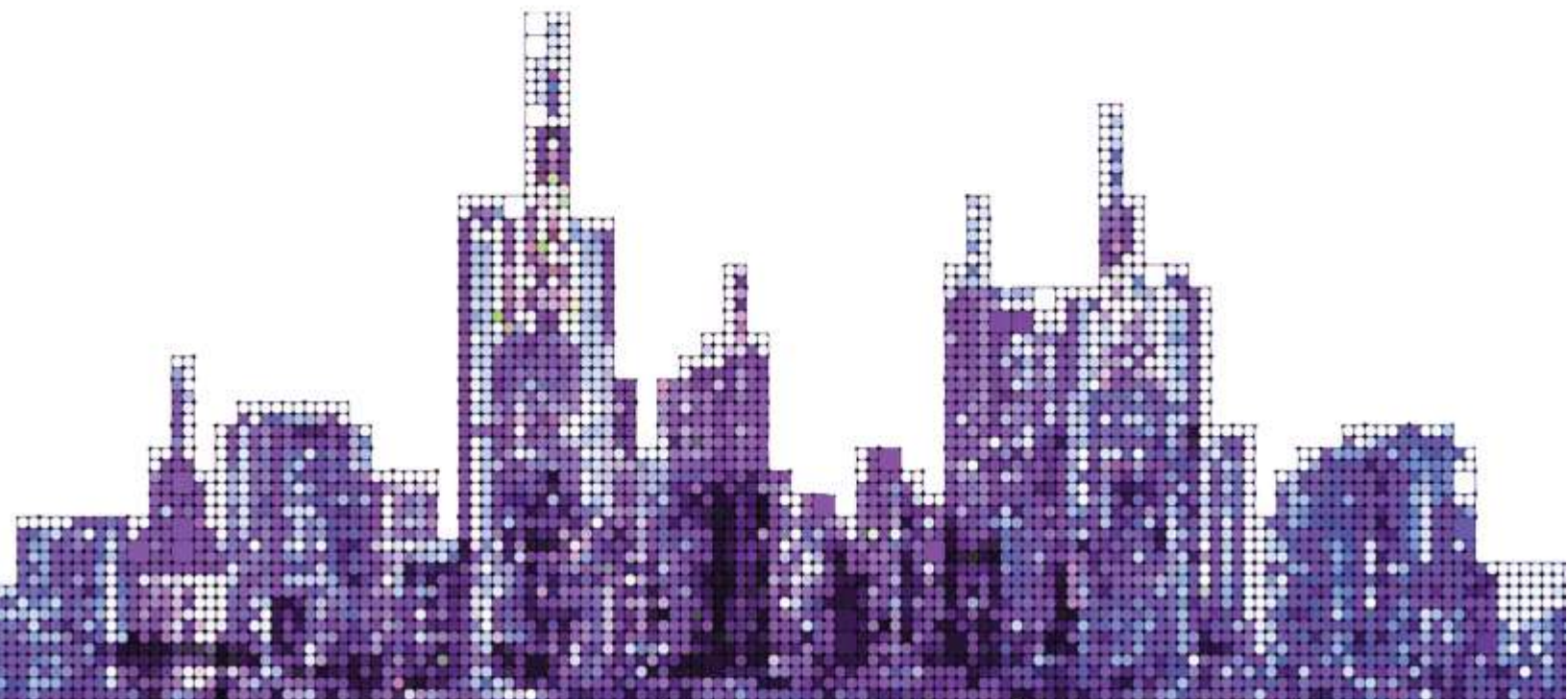# Multi-agent Simulation-based Virtual Test Bed Ecosystem: MATSim-NYC

May 2020

**C2SMART Center** is a USDOT Tier 1 University Transportation Center taking on some of today's most pressing urban mobility challenges. Using cities as living laboratories, the center examines transportation problems and field tests novel solutions that draw on unprecedented recent advances in communication and smart technologies. Its research activities are focused on three key areas: Urban Mobility and Connected Citizens; Urban Analytics for Smart Cities; and Resilient, Secure and Smart Transportation Infrastructure.

Some of the key areas C2SMART is focusing on include:

**Disruptive Technologies**

We are developing innovative solutions that focus on emerging disruptive technologies and their impacts on transportation systems. Our aim is to accelerate technology transfer from the research phase to the real world.

**Unconventional Big Data Applications**

C2SMART is working to make it possible to safely share data from field tests and non-traditional sensing technologies so that decision-makers can address a wide range of urban mobility problems with the best information available to them.

**Impactful Engagement**

The center aims to overcome institutional barriers to innovation and hear and meet the needs of city and state stakeholders, including government agencies, policy makers, the private sector, non-profit organizations, and entrepreneurs.

**Forward-thinking Training and Development**

As an academic institution, we are dedicated to training the workforce of tomorrow to deal with new mobility problems in ways that are not covered in existing transportation curricula.

Led by the New York University Tandon School of Engineering, C2SMART is a consortium of five leading research universities, including Rutgers University, University of Washington, the University of Texas at El Paso, and The City College of New York.

c2smart.engineering.nyu.edu

# Virtual Test Bed Ecosystem:

# MATSim-NYC

Joseph Y.J. Chow
*New York University*
ORCID: 0000-0002-6471-3419

Kaan Ozbay
*New York University*
ORCID: 0000-0001-7909-6532

Yueshuai He
*New York University*
ORCID: 0000-0002-5794-7751

Jinkai Zhou
*New York University*

Ziyi Ma
*New York University*

Mina Lee
*New York University*

Ding Wang
*New York University*

Di Sha
*New York University*

# Disclaimer

# Acknowledgements

## Executive Summary

To grapple with emerging technologies, city agencies need to evaluate operational scenarios imposed by private sector (e.g. what is the impact of e-hail ride-sourcing on traffic congestion?) or when considering what-if scenarios related to new operating policies. This is especially important because technologies companies developing public products need to gain approval from public agencies before they can deploy in that region. As such, public agencies need to evaluate the product's impact on the community. Transportation products like policies and operating technologies face different challenges than conventional technologies because of their public nature. Transportation technologies deployed to the field can be both financially and socially costly, as unproven technologies may end up costing lives if something goes wrong. Furthermore, even a successful deployment in one city may not be indicative that the same technology can work well in another city because each city is a different market. Prototyping serves to verify that a technology works, but it does not consider how the technology may impact a community given the behavior of its population. This gap in the innovation process for transportation technologies suggests a need for a deployment testing framework that falls between prototyping and field piloting. Existing tools like NYBPM are designed more for long term capital planning than for quick response evaluation of operating policies introduced by emerging transportation technologies, which are often dynamic and impact travelers' travel preferences throughout the day. Congestion pricing, algorithms for microtransit or bikeshare rebalancing, electric vehicle fleets with dynamic fast charging activities all impact travelers' choices throughout the day, which in turn impact the dynamics of traffic congestion throughout the day. These interactions are currently not addressed by any existing tools in NYC, nor in most cities around the world.

One of the missions of C2SMART is to help cities around the country better understand the transferability of transportation technologies. For this purpose, we initiated two yearlong projects from 2018 – 2020 to initiate a new virtual test bed ecosystem:

- 2018 – 2019: Phase I: Open Source Multi-Agent Virtual Simulation Testbed
- 2019 – 2020: Phase II: Development and Tech Transfer of Multi-Agent Simulation Testbed

This report covers the findings of both years' projects. The objective of these two projects is to develop an initial architecture and virtual test bed that can be replicated in future projects to other cities in the C2SMART consortium and partners. The vision is for a "Network of Living Labs",

which is tentatively dubbed as C2SMART's "NOLL-Edge" system. Its goal is to be used by city agencies to evaluate emerging technologies and operating policies using a consistent platform so that their effects can be quantified. In the long term, cities may opt to use this test bed as a means of certification for policies and technologies (e.g. NOLL-Edge-certified that policy A can achieve X% welfare improvement in NYC or reduce congestion by Y% for population segments 1, 2, 3, etc.). The test bed system is integrated within an Urban Data Observatory. Users of the virtual test bed are divided into 3 groups: (a) agencies that want to evaluate a scenario; (b) technology companies that want to submit their technologies for deployment testing; (c) research partners who want to conduct research using data from the system. Users need to be able to query data, define scenarios with C2SMART for which comparisons to baseline scenario are made, submit extensions that capture new technologies to use in a scenario, or develop a new model that better fits the needs of the scenario to be evaluated.

We developed an initial test bed for NYC using MATSim, a Multi-Agent Transportation Simulation. MATSim models transportation networks using a mesoscopic simulation based on cellular automata. It is open source and many extensions have been quickly developed for it to handle a wide assortment of policy needs: autonomous vehicles, emissions modeling, parking, freight, electric vehicles, bikeshare, etc. MATSim makes use of a synthetic population which is useful for modeling heterogeneous population segments. It incorporates a day-to-day adjustment process that can reflect learning from the population to achieve a social equilibrium under each technology scenario.

Based on this overarching goal, we set out on these two projects with the following set of objectives:

- Create an underlying synthetic population for NYC for a recent base year (2016) that includes key emerging modes like Citi Bike and for-hire vehicles (FHVs) like Uber/Lyft/Via;
- Construct, calibrate, and validate a MATSim model of NYC using the synthetic population;
- Use the synthetic population and MATSim models to evaluate a set of scenarios for which existing tools are not equipped:
  - The now-defunct plan to establish an Amazon headquarters in Long Island City and the impact resulting from trips taken by professional service employees to that area;
  - Citi Bike expansion plan and the resulting effect on travelers, which is not currently modeled as a mode in any existing travel demand tool for NYC;

- o Congestion pricing for Manhattan, and its impact on traffic propagation into and out of Manhattan by time of day;
  - o Brooklyn-Queens Connector (BQX), a proposed streetcar service for which there is no broad consideration of demand for its service at a citywide level.
- Exploration of other features of MATSim:
  - o Mobility-on-demand-based autonomous vehicle fleets;
  - o Bike-share;
  - o Multimodal travel;
  - o More realistic traffic flow modeling on the links.

We used the PopGen 2.0 (MARG,2016) to generate the representative synthetic population while controlling and matching both household-level and person-level attributes. We generated a population of 8.24 million people for the base year of 2016, compared to a total true population of 8.34 million people. There was an average of 4% difference between the synthetic population and the Longitudinal Employer-Household Dynamics 2016 data. Travel agendas were replicated from the 2010/2011 Regional Household Travel Survey, minus the mode for each trip. Over 30 million trips were synthesized. Modes were synthesized using a mode choice model.

A tour-based nested logit model was developed and calibrated using the 2010/2011 RHTS for driving, walking, carpool, public transit (both subway and bus), taxi, and bike. For-hire vehicles (e.g. e-hail, ridesourcing) and Citi Bike modes were estimated by perturbing the existing model with new modes to fit count data in 2016 using least squares. An additional smartphone ownership choice model was estimated to use as an attribute or alternative availability indicator. The model was estimated for two population segments: people living in Manhattan and those living outside Manhattan. The value of time for the Manhattan segment was estimated to be $29/h.  The model was validated against the 2017 Citywide Mobility Survey from the New York City Department of Transportation (NYC DOT), and found to fit well.

The completed synthetic population was then fed into MATSim simulation along with data for the road network from OpenStreetMap, transit schedule from GTFS, and other simulation-level configuration parameters. Gateway trips were added to account for origins outside of NYC entering through the city, which account for 1.18M additional population and 3.04M trips. The nested logit model parameters were converted to equivalent multinomial logit model parameters to fit MATSim's score function framework. The road network was calibrated further by speed and capacity, differentiated by time of day as well as by arterial or freeway. The speeds were initially calibrated against INRIX data while the capacities were calibrated against the hourly

traffic counts of 19 bridges and tunnels around the city. The resulting model, called MATSim-NYC, had a relative difference on average of 7.2% for the freeways and 17.1% for the arterials. The simulated screenlines along the bridges and tunnels had an average relative difference of 25.9% for the Hudson screenline and 2.6% for the East River screenline, with an overall average relative difference over different time periods of 10.3%. Validation of MATSim-NYC was conducted using transit ridership across ten of the highest volume ridership and hourly volumes of 15 major locations in NYC. The transit stations show a difference in total daily ridership of 8% while the median difference for the traffic volumes is 29%.

The calibrated synthetic population and MATSim-NYC model were then applied to create a baseline scenario from which we analyzed four different scenarios. The first two scenarios are analyzed using the synthetic population. Scenario 1 looked at building the office space for the Amazon HQ in Long Island City as originally planned, showing that it would increase morning peak hour trips from 5000 to 8000 while expanding taxi and FHV demand to/from that location by more than four times. Scenario 2 studies the Citi Bike expansion which predicts the number of daily trips would increase from 47K daily trips to 91K daily trips.

The latter two scenarios are analyzed using MATSim-NYC. Scenario 3 is the congestion pricing plan for NYC. A $9.18 peak period pricing plan analyzed by RPA is also looked at. Our model predicts twice the number of cars shifted away (127,000) than RPA (59,000); most of which are absorbed by transit. Revenues are consistent. In addition, MATSim-NYC allows us to measure the impact on consumer surplus, suggesting benefits for Manhattanites that are on average 54% higher than for non-Manhattanites. This warrants more careful redistribution of the pricing revenue toward outer boroughs transit services. We can also see to which modes the trips shift: 15% of car trips shift to transit and 10% shift to FHV and taxi. Scenario 4 looks at the Brooklyn-Queens Connector (BQX) and predicts a higher daily ridership (112K) than the original BQX study (50,000). We also predict a peak load during morning peak hours of 1400 passengers/hour along with a prediction of 16% of BQX riders shifting from car mode (18K cars).

A summary of other extensions are also provided: we developed more realistic traffic flow models within the simulation; we investigated the use of an autonomous mobility-on-demand (AMoD) extension for MATSim-NYC; we reviewed tools available for handling multimodal routing and bike-share in MATSim; and we planned out next steps for integrating the test bed in the urban data observatory.

The projects have resulted in presentations given at University of Maryland, ETH Zurich, and ICTPA, as well as a webinar covering application to congestion pricing and COVID-19. Four papers were prepared directly from the tool development; several other papers were also prepared in conjunction while studying multimodal transport and emerging technologies (12 in total). The work has supported two other projects at C2SMART, supported several PhD students for portions of their dissertations, several MS theses, a Center for Urban Science and Progress (CUSP) capstone, the The NYU Tandon School of Engineering's Applied Research Innovations in Science and Engineering (ARISE) program, graduate and undergraduate courses by Professor Chow, the NYU Tandon Research Expo presented to the public, and integrated into courses and training for NYCDOT and ITS-NY members.

# Table of Contents

## List of Figures

## List of Tables

## Section 1: Introduction

### 1.1. Background

Cities are facing a growth in new technologies and operational models due to the rise of the Internet of Things (IoT) within the "smart cities" context. A fine example of the impact this paradigm shift has on mobility options is shown in Figure 1 under a Mobility-as-a-Service (MaaS) paradigm. Whereas traditional transportation planning tools focused on evaluation of roadway infrastructure and public transit alternatives, emerging mobility services and technologies play a much bigger role (Chow, 2018).
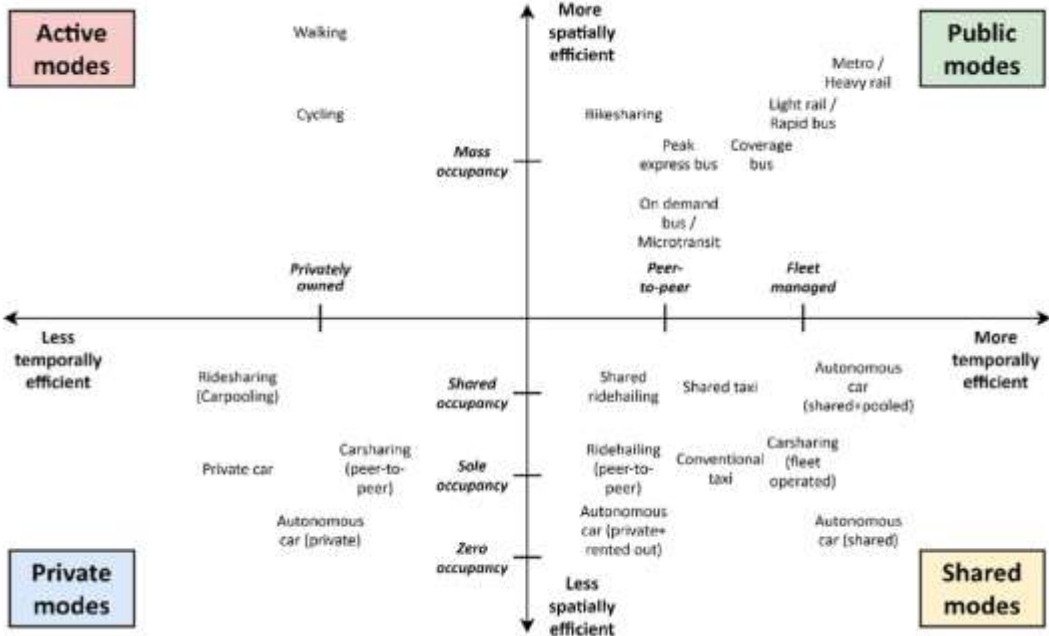


**Figure 1. Spectrum of modes available in a MaaS paradigm (source: Wong et al., 2020).**

To grapple with these emerging technologies, city agencies need to evaluate operational scenarios imposed by private sector (e.g. what is the impact of e-hail ride-sourcing on traffic congestion?) or when considering what-if scenarios related to new operating policies. This is especially important because technologies companies developing public products need to gain approval from public agencies before they can deploy in that region. As such, public agencies need to evaluate the product's impact on the community.

How should government agencies test such products? For most engineered products, the evaluation and testing phases of a product out of research and development is either prototyping or deployment testing in the field. An illustration of these kinds of efforts in deployment testing is shown in Figure 2, which shows a set of pilot public-private partnership projects in various parts of the country. It includes several funded by the Federal Transit Administration to test the deployment of new technologies and operating policies, called the MOD (mobility-on-demand) Sandbox program.
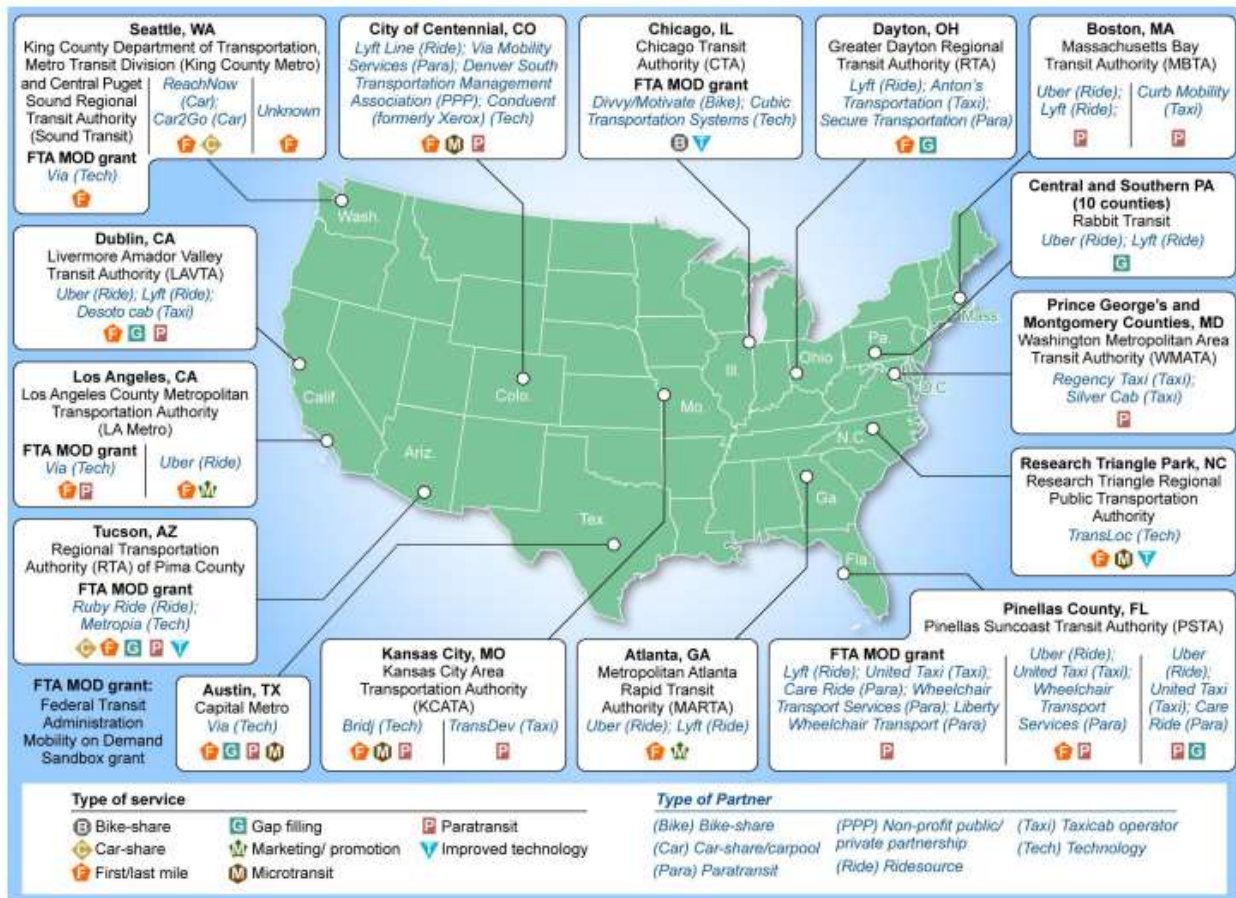


**Figure 2. Selected transit partnerships, several of which are from the MOD Sandbox program (source: GAO, 2018).**

However, transportation products like policies and operating technologies face different challenges than conventional technologies because of their public nature. As illustrated in Figure 3, transportation technologies deployed to the field can be both financially and socially costly, as unproven technologies may end up costing lives if something goes wrong. Furthermore, even a successful deployment in one city may not be indicative that the same technology can work well

in another city because each city is a different market. Prototyping serves to verify that a technology works, but it does not consider how the technology may impact a community considering the behavior of its population. This gap in the innovation process for transportation technologies suggests a need for a deployment testing framework that falls between prototyping and field piloting. The lack of a consistent deployment modeling and testing phase between prototyping and deployment pilot can lead to higher failure rates in emerging technologies. As we have seen, companies like Chariot, Bridj, ReachNow, Bird, among others (see Chow, 2018, for other examples), have all failed to operate sustainably. An ex post analysis of Kutsuplus microtransit suggests the operating conditions might not have been adequate to maintain such services (Haglund et al., 2019).
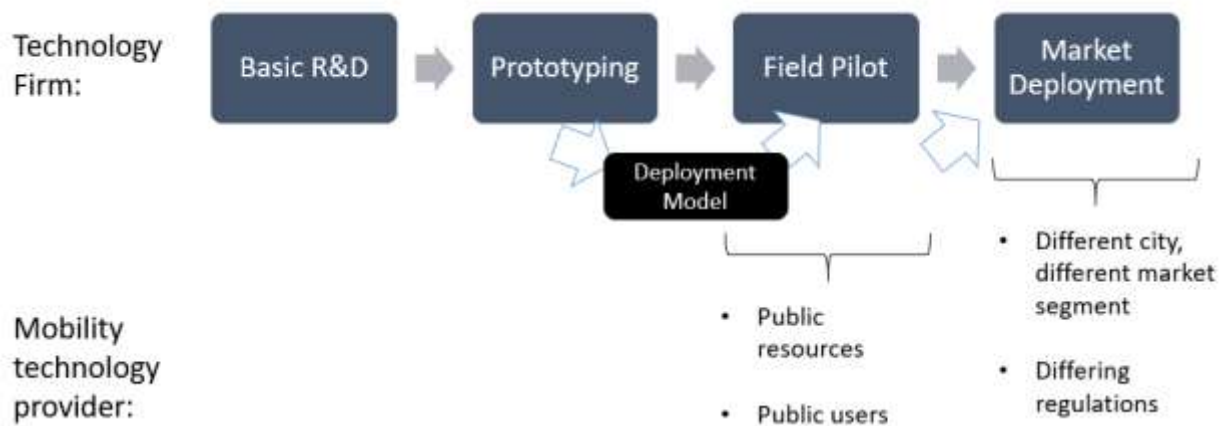


**Figure 3. Illustration of unique aspects of innovation process for transportation technologies.**

As an example, consider New York City. When new mobility providers wish to enter the market, they need approval from city officials. The officials have at their disposal a limited set of tools to evaluate the impact of the technology on the city. One prominent tool is the regional travel demand model from the New York Metropolitan Transportation Council (NYMTC), called the New York Best Practice Model (NYBPM). The NYBPM study area includes 28 counties of New York, New Jersey and Connecticut and both road and public transit network are incorporated. It took about two years (from mid-May 2013 to mid 2015) to update the base year of the model to 2010. The 2012 base year update was expected to be ready by end of 2018. Even the latest version of NYBPM (2012) is too old to capture the dramatic growth of FHV since 2015. NYBPM is designed more for long term capital planning than for quick response evaluation of operating policies introduced by emerging transportation technologies which are often dynamic and impact travelers' travel preferences throughout the day.

Another available tool is the Balanced Transportation Analyzer (BTA) developed by Nurture Nature Foundation (NNF). It is an intricate spreadsheet model that can analyze the impacts of transportation fares or other variables. The Regional Planning Association (RPA) published a report about the congestion pricing analysis in Manhattan using this model. However, this model does not capture spatiotemporal interactions within the city and can only provide a city-level assessment of a congestion pricing plan.

Congestion pricing, algorithms for microtransit or bikeshare rebalancing, electric vehicle fleets with dynamic fast charging activities all have one thing in common: they impact travelers' choices throughout the day, which in turn impact the dynamics of traffic congestion throughout the day. These interactions are currently not addressed by any existing tools in NYC, nor in most cities around the world.

## 1.2. Research objectives

One of the missions of C2SMART is to help cities around the country better understand the transferability of transportation technologies. For this purpose, we initiated two yearlong projects from 2018 – 2020 to initiate a new virtual test bed ecosystem:

- 2018 – 2019: Phase I: Open Source Multi-Agent Virtual Simulation Testbed
- 2019 – 2020: Phase II: Development and Tech Transfer of Multi-Agent Simulation Testbed

This report covers the findings of both years' projects. The objective of these two projects is to develop an initial architecture and virtual test bed that can be replicated in future projects to other cities in the C2SMART consortium and partners. The vision is for a "Network of Living Labs", which is tentatively dubbed as C2SMART's "NOLL-Edge" system. Its goal is to be used by city agencies to evaluate emerging technologies and operating policies using a consistent platform so that their effects can be quantified. In the long term, cities may opt to use this test bed as a means of certification for policies and technologies (e.g. NOLL-Edge-certified that policy A can achieve X% welfare improvement in NYC or reduce congestion by Y% for population segments 1, 2, 3, etc.). A conceptual use case diagram of the system is provided in Figure 4.
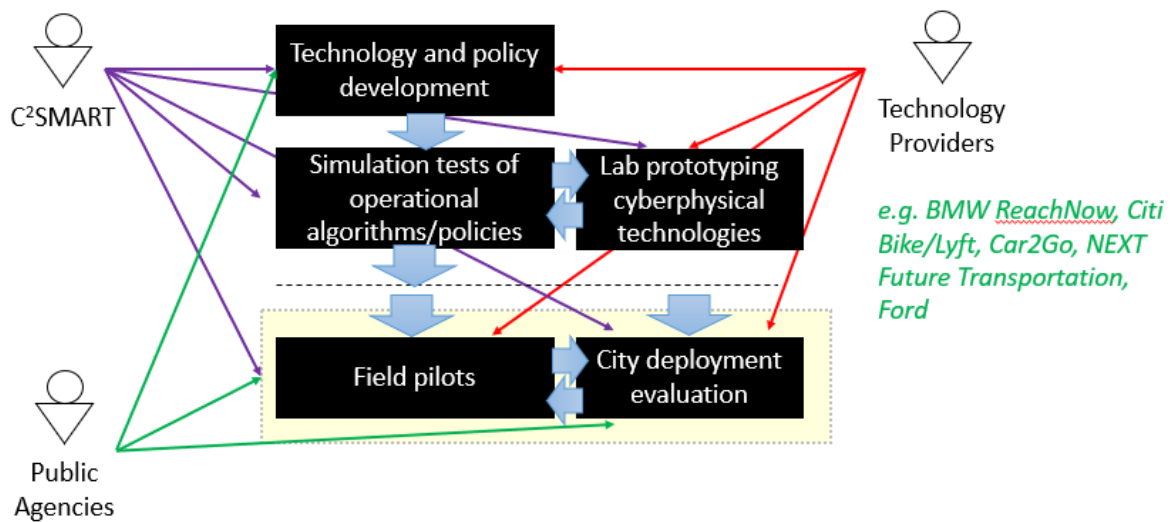
**Figure 4. Conceptual use case diagram of NOLL-Edge system.**

The test bed system is integrated within an Urban Data Observatory. Users of the virtual test bed are divided into 3 groups: (a) agencies who want to evaluate a scenario; (b) technology companies that want to submit their technologies for deployment testing; (c) research partners who want to conduct research using data from the system. Users need to be able to query data, define scenarios with C2SMART for which comparisons to baseline scenario are made, submit extensions that capture new technologies to use in a scenario, or develop a new model that better fits the needs of the scenario to be evaluated. An illustrative screenshot is shown in Figure 5 and a screenshot of a data query interface is shown in Figure 6.
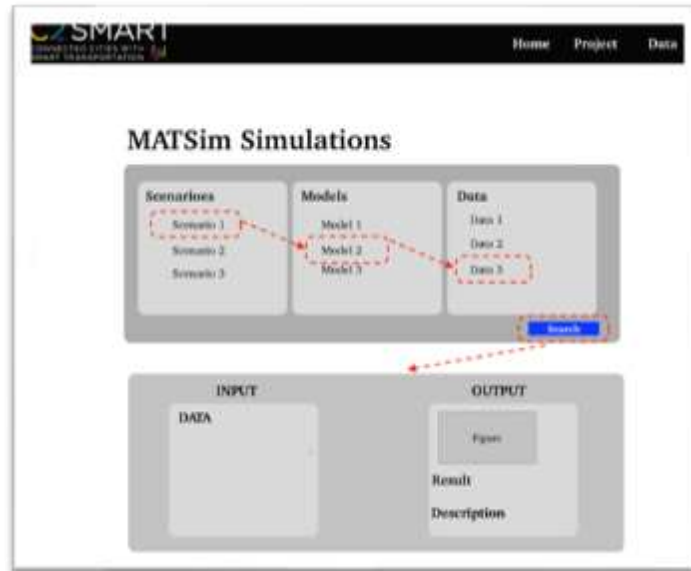
**Figure 5. Illustrative screenshot of the MATSim interface.**



**Figure 6. Illustrative screenshot of OD data query tool (NTA mode).**

The requirements for the virtual test bed system are listed as follows:

- It needs to recognize dynamic traffic propagation to capture traffic technologies and policies like congestion pricing;
- It needs to recognize activity scheduling behavior of travelers (see Kang et al., 2013);

- It needs to recognize different segments of travelers in the population, e.g. low and high income, age groups, residents of different socioeconomic backgrounds;
- It needs to be flexible enough to adapt to new emerging technologies.

Based on these requirements, we chose to develop the initial test bed for NYC using MATSim, a Multi-Agent Transportation Simulation. MATSim models transportation networks using a mesoscopic simulation based on cellular automata. It is open source and many extensions have been quickly developed for it to handle a wide assortment of policy needs: autonomous vehicles, emissions modeling, parking, freight, electric vehicles, bikeshare, etc. MATSim makes use of a synthetic population which is useful for modeling heterogeneous population segments. It incorporates a day-to-day adjustment process that can reflect learning from the population (see Djavadian and Chow, 2017a,b) to achieve a social equilibrium under the technology scenario.

It also has many limitations. The base platform does not directly incorporate freight populations, nor parking, nor easily account for shared lanes between buses and passenger vehicles. It doesn't handle dynamic tolling, bikeshare, or multimodal trips. This is more reason to conduct a study to test its capabilities and limitations in modeling different policies and emerging technologies.

Based on this overarching goal, we set out on these two projects with the following set of objectives:

- Create an underlying synthetic population for NYC for a recent base year (2016) that includes key emerging modes like Citi Bike and for-hire vehicles (FHVs) like Uber/Lyft/Via;
- Construct, calibrate, and validate a MATSim model of NYC using the synthetic population;
- Use the synthetic population and MATSim models to evaluate a set of scenarios that existing tools are not equipped to evaluate:
  - The now-defunct Amazon headquarters location plan in Long Island City and the impact of increased trips to that area by professional service employees;
  - Expansion plan by Citi Bike, not currently modeled as a mode in any existing travel demand tool for NYC, and the resulting effect on travelers;
  - Congestion pricing for Manhattan, which requires evaluating its impact on traffic propagation into and out of Manhattan by time of day;
  - Brooklyn-Queens Connector (BQX), a proposed streetcar service for which there is no broad consideration of demand for its service at a citywide level.
- Exploration of other features of MATSim:
  - Mobility-on-demand-based autonomous vehicle fleets;

- o Bike-share;
- o Multimodal travel;
- o More realistic traffic flow modeling on the links.

## 1.3. Organization of report

The rest of the report is organized as follows. Section 2 provides an overview of MATSim and agent-based modeling needed to work with the subsequent sections. Section 3 introduces the development of the eight-million synthetic population. The calibration of MATSim baseline model is demonstrated in Section 4 and the results of scenario analyses are discussed in Section 5. Section 6 presents the findings of the exploratory efforts on other features of MATSim as well as an overview of the Urban Data Observatory under which the NOLL-Edge system would reside. Section 7 concludes the report and summarizes the tech transfer from this project, which includes future plans to make the system accessible to stakeholders and further grow the system.

### 2.1 Agent-Based Modeling and Simulation

Agent-Based Modeling and Simulation (ABMS) (von Neumann, 1966; Bonabeau, 2002) can be used to model complex heterogeneous agents with interaction rules and agent learning. ABMS has been applied to many problems in the transportation area (see Dia, 2002; Hidas, 2002; Zhang, 2006; Rieser et al., 2016). Macal and North (2006) classified the applications of ABMS into two categories: "Small, elegant, minimalist models" and "Large-scale decision-support systems". The latter is more suitable to facilitate the emerging needs of policymakers. Djavadian and Chow (2017a,b) demonstrated how agent-based simulation can be used to capture market equilibration for dynamic transportation systems, many of which feature in MaaS systems. An illustration of this framework is shown in Figure 7. In the figure, FTS stands for "flexible transport systems" which represent dynamic service systems that may include user and operator decisions. The framework is shown to reach a stochastic user equilibrium for populations that are sampled sufficiently (Djavadian and Chow, 2017a), which provides a basis for agent-based simulations of such transportation systems.
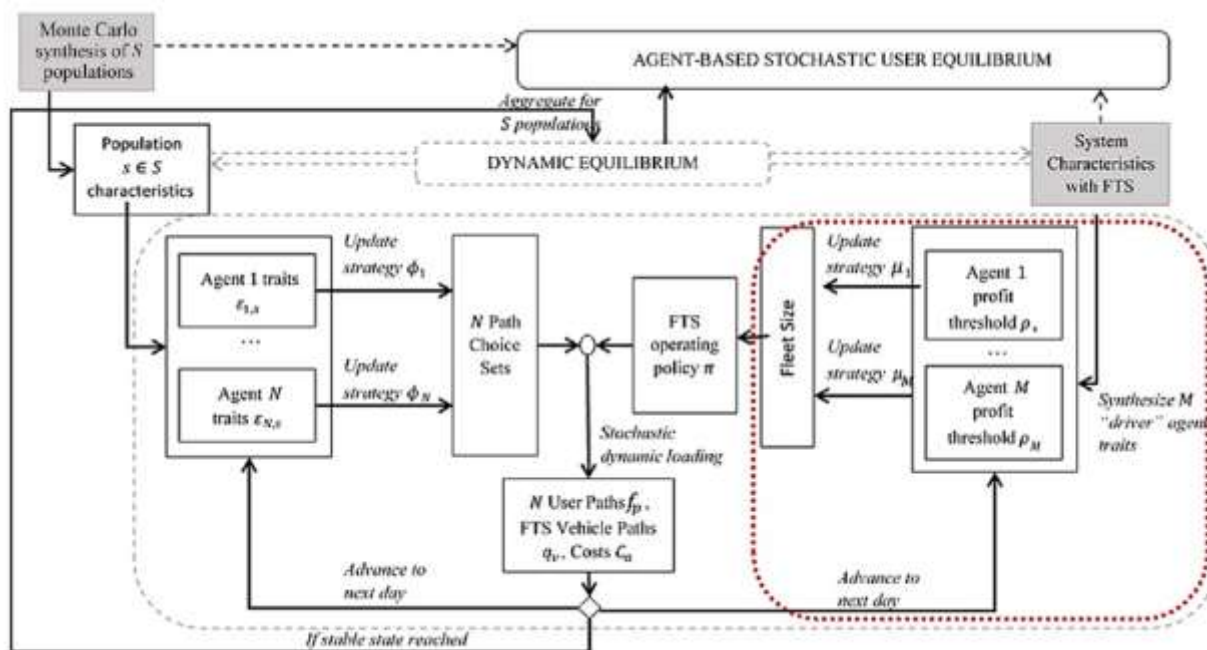


**Figure 7. Framework for day-to-day adjustment processes for evaluating market equilibrium of dynamic transportation systems with user and operating learning (source: Djavadian and Chow, 2017b).**

There are several well-known ABMS platforms designed to support decision-making, including but not limited to Transportation Analysis and Simulation System (TRANSIMS) (Nagel et al., 1999, Multi-Agent Transport Simulation Toolkit (MATSim) (Balmer et al., 2009), Sacramento Activity-Based Travel Demand Simulation Model (SACSIM) (Bradley et al., 2012) Simulator of Activities, Greenhouse Emissions, Networks, and Travel (SimAGENT) (Goulias et al., 2011), and Polaris (Auld et al., 2016), SimMobility (e.g. Nahmias-Biran et al., 2019). TRANSIMS was a first-generation tool developed by the Federal Highway Administration (FHWA), after which its creators took the lessons learned from it to produce the next generation tool MATSim.

These agent-based simulation tools typically assume a single population of agents, so the results of their simulations may not necessarily converge toward a theoretical stochastic user equilibrium described in Djavadian and Chow (2017a), but they can provide an approximation especially given a large enough synthetic population that allows for a sufficiently broad range of agents to be simulated. To illustrate, we ran MATSim over four different runs at 4% of population. As shown in Table 1, the sample standard deviation over the four runs are quite small, suggesting that only one run is necessary.

**Table 1. Sensitivity tests of stability of MATSim predicted trips per mode over four runs**

|  | car | carpool | transit | taxi | bike | walk | Citi Bike | FHV |
|---|---|---|---|---|---|---|---|---|
| **Mean** | 28567 | 2516 | 208042 | 19907 | 8168 | 126431 | 1022 | 18497 |
| **Std dev.** | 190 | 43 | 323 | 219 | 61 | 97 | 37 | 222 |

## 2.2 MATSim Overview

MATSim is an open-source simulation toolkit implemented in Java. It has three desirable features that make it unique among other agent-based simulations. The first is the use of a synthetic population that includes activity schedules so that simulation incorporates activity scheduling behavior. The role of MATSim as a simulation of activity scheduling is discussed at great length in Chapter 4 of Chow (2018). The issue in many activity scheduling models is the lack of sensitivity to spatial temporal constraints reflected at a large scale in the population, a drawback discussed in Chow and Recker (20120 and Chow and Djavadian (2015). MATSim

provides a feedback loop by using a day-to-day adjustment process, although the adjustment process is simplified with a heuristic (a genetic algorithm) and the use of only a single population.

The second desirable feature is that MATSim can simulate large-scale scenarios using a spatial queue model (Cetin et al., 2003) to simulate the traffic dynamics instead of car-following and lane-changing models (Zheng et al., 2013). To shorten the computation time, MATSim also adopts parallel computation for the spatial queue model. However, there are some shortcomings of the spatial-queue model in MATSim. First, the backward wave speed may not be realistic. Since vehicles leave the link one by one as a queue, when the previous vehicle leaves the link, the whole link would be available immediately and the backward wave speed is nearly the length of the link per time step. The intra-link interactions among vehicles are ignored. Second, factors like traffic signal, pedestrians, and on-street parking are ignored by the default MATSim model. In a complex urban road network like NYC, traffic flows are significantly affected by those factors. These two shortcomings are addressed in the project.

Another advantage of MATSim is its numerous extensions as an open-source platform, which makes it easier for users to simulate and evaluate different scenarios. There are many applications of MATSim around the world, including Berlin (Neumann, 2016; Ziemke, 2016), Zurich (Rieser-Schü·ssler et al., 2016), Singapore (Erath and Chakirov, 2016) among others. These applications prove that MATSim is suitable for analyzing the complex urban transportation system in large cities. MATSim has also been used to evaluate several emerging technologies, including the following examples:

- Autonomous vehicle fleet (Hörl et al., 2019)
- Carshare (Ciari et al., 2016)
- Urban air mobility (Rothfield et al., 2018)
- Demand-responsive transit (Cich et al., 2017)
- MaaS (Becker et al., 2020)

As an agent-based simulation, MATSim can capture the behavior of each agent and the interaction between agents and transportation system. Each agent refers to an individual traveler. Traveler behavior is represented by a series of activities, travel modes and routes. MATSim uses an iterative framework for simulation, as shown in Figure 8. The goal of the iterative framework is to find the equilibrated state of the system. The overall simulation procedures are:

- Put the agents with the initial travel plans into MATSim and simulate their mobility in the physical system.

- Calculate the score (utility) of each agent's executed plan.
- Randomly select a certain proportion of agents and mutate their plans. Go back and re-run the simulation until the agents' scores converge.
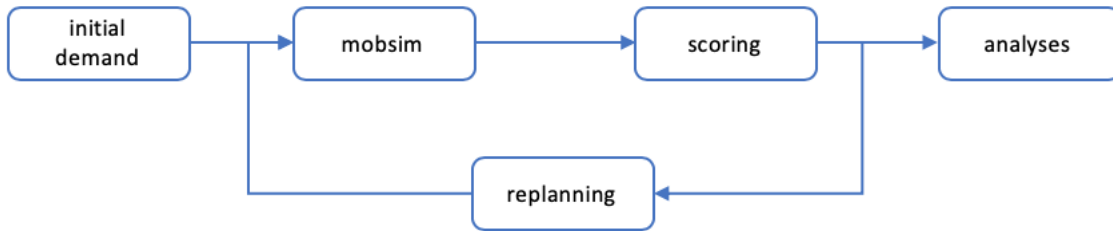


**Figure 8. Framework of simulation in MATSim (Horni et al., 2016).**

The output of MATSim has very high resolution. It contains the executed plan of all the agents. Many useful results can be extracted from this output, such as:

- Aggregated-level mode share
- Individual mode shift in a specific scenario
- Departure time distributions across a day
- Trip travel distance distributions per mode
- Average hourly speed distribution across a day per link
- Transit ridership profile per line
- Passenger flow distribution per station
- Traffic count at specific link

## Section 3: Synthetic population

There are three major steps to develop a synthetic population for NYC: population synthesis, agenda assignment and travel mode determination. All three steps are introduced in detail in the rest of this section.

### 3.1 Population synthesis

We used the PopGen 2.0 (MARG,2016) to generate the representative synthetic population while controlling and matching both household-level and person-level attributes. PopGen 2.0 uses an enhanced iterative proportional updating (IPU) algorithm (Konduri,2016) to control the distribution of population attributes at different spatial layers simultaneously.

The population attributes are distributed in both county level as well as Traffic Analysis Zone (TAZ) level in the NYC model. Available attributes are collected from the American Community Survey (ACS), NYMTC 2040 Socioeconomic and Demographic (SED) Forecasts, and Longitudinal Employer-Household Dynamics 2016 (LEHD), as shown in Table 2. Some data from ACS and LEHD are based on the Blockgroup spatial resolution, which is inconsistent with our default TAZ spatial resolution. We matched the Blockgroup to TAZ to keep the consistency of the data. If one Blockgroup is shared by more than one TAZ, we assign the attributes from ACS and LEHD to the TAZ according to its proportion of area among the overlapped TAZs.

We generated a population of 8.24 million people for the base year of 2016 with the attributes given in Table 2, compared to a total true population of 8.34 million people (SED, 2016). This resulted in 30,991,820 average daily trips made by the synthetic population in 2016. The computation time was 12 minutes and 35 seconds on an Intel Xeon 3.5 GHz with 125 GB RAM.

The distribution of employment industry proportion from the synthetic population was compared to LEHD data shown in Figure 9. The Educational services industry has the largest difference as 9% lower, with the average difference 4%. The distribution of personal information was also validated to SED forecast data (Table 3).

**Table 2. Attributes available from ACS, LEHD and SED data**

| Data Source | Attributes | Description |
|---|---|---|
| ACS | Person Age | Age group of the person |
| | Person School Enrollment Status | If student, person's academic level |
| | Person Gender | Male or female |
| | Household Size | Number of people in the household |
| | Household Income | Income group of the household |
| | Household Car Ownership | Number of cars owned by the household |
| LEHD | Person Work Industry | If working, person's employment industry according to NAICS |
| SED | Employment | Worker or not |
| | Total Population by TAZ | Resident population in TAZ |
| | Total Population By County | Resident population in County |
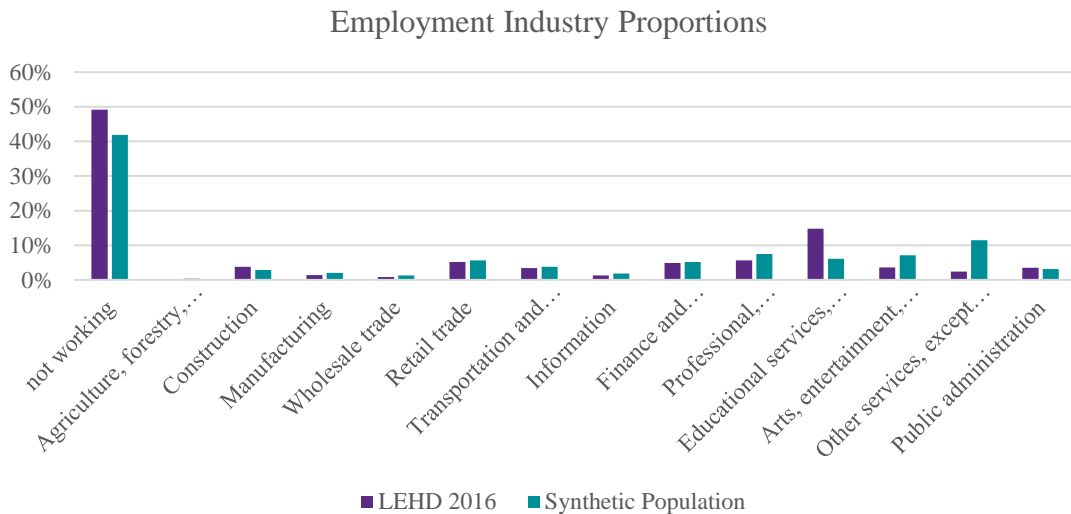


**Figure 9. Comparison of the synthesized and LEHD distributions of the population employment industry.**

**Table 3. Validation results of the synthetic population comparing with SED data by zone**

| Attributes | Maximum % Difference | Mean % Difference |
|---|---|---|
| Person Age | 5 | 2 |
| Person School Enrollment Status | 9 | 4 |
| Person Gender | 6 | 4 |
| Person Work Industry | 4 | 3 |
| Employment | 7 | 4 |
| Total Population by TAZ | 3 | 2 |
| Total Population by County | 3 | 2 |

## 3.2 Agenda assignment

The travel agenda of a person consists of a series of activities and trips. The agents' agendas have multiple dimensions, such as activity purpose, destination choice, departure time choice, and duration choice. We only model tour-based mode choice; the other dimensions are simply assigned from the 2010/2011 Regional Household Travel Survey (RHTS), which includes 35,207 agendas. There are more than 30 million trips in total and 3.5 trips per capita. We assigned RHTS agendas to the synthetized population using socio-demographic information. There are two assignment considerations: home location and occupation.

Generally, every person in the synthetic population is assigned an agenda of a RHTS sample individual from the same TAZ with the same type of occupation, but some TAZs have few or no responses. The sampling pool for agents drawn from TAZs with less than 15 sample agendas is extended to the Public Use Microdata Area (PUMA) level where the TAZ belongs.

Travel patterns are also dependent on the agent's occupation. Four categories of occupation are defined: K-12 (kindergarten to 12th grade) students, university students, workers, and retiree/unemployed. K-12 students only receive school agendas, university students receive university agendas, workers receive work agendas, and retirees and the unemployed receive only secondary activity agendas.

Based on these two criteria, every person is given an agenda. If an agenda is drawn from the PUMA level, the start location for the first trip of the day and the end location of the last trip of the day is adjusted to the home location of its agent. A mode choice model is proposed in the

next section to simulate the modes chosen for each trip in the agendas of the synthetic population.

## 3.3 Travel mode determination

### 3.3.1 Model specification

A tour-based nested logit model is proposed to determine the travel mode choices of the synthetic population. A tour consists of a series of linked trips of which the beginning of the first trip and the end of the last trip are the same location. Here we assume all tours are independent from each other. Furthermore, some long tours consist of a series of "sub-tours". A sub-tour is part of a tour starting and ending at the same location. The tours and subtours are illustrated in Figure 10, which shows the possibility for multiple tours from home (H). Each home-based tour is decided as car or non-car. For non-car tours, the modes of each trip are decided independently. The availability of car mode in a subtour (e.g. A1-A3-A1) depends on whether the greater tour used a car or not. The tour-based design captures the interdependency among trips and the car consistency across a tour, compared to the traditional trip-based model.
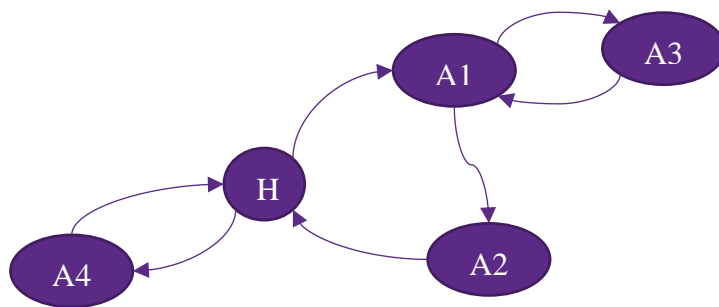
**Figure 10. Illustration of three tours from an individual: two home-based tours (H-A1-A2-H, H-A4-H), one non-home-based subtour (A1-A3-A1).**

The structure of the nested logit model is shown in Figure 11. The upper nest determines driving or not in the tour level, while the lower nest determines the mode choice in the trip level

based on the choice of non-driving in the upper level. The model is initially estimated from the 2010/2011 RHTS ignoring modes 6 and 7. This difference reflects the For-Hire-Vehicle (FHV) and Citi Bike, which are not incorporated by RHTS.
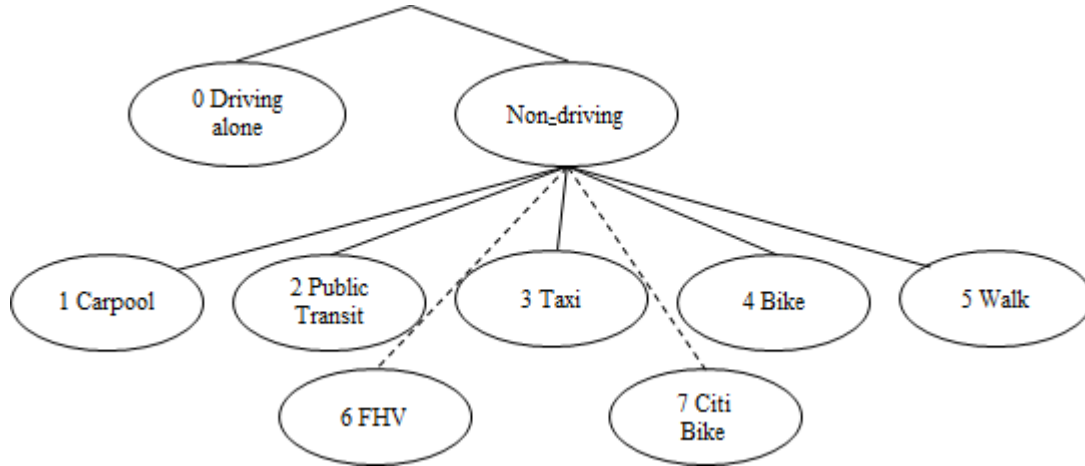


**Figure 11. Structure of nested logit model.**

In the driving nest $N_1$, there is only driving mode for the whole tour. In the non-driving nest $N_2$, we denote a choice set $J = \{1,2,3,4,5\}$ corresponding to non-driving modes labeled in Figure 11.

To handle the difference in units between the lower level (per trip) and upper level (per tour), the expected tour-level utility of $N_2$ is calculated according to Eq. (3.1).

$$E[V_{N_2,i}] = \frac{1}{\mu} \sum_{k=1}^{K_i} \ln \left( \sum_{j=1}^{J} e^{\mu V_{ijk}} \right) \tag{3.1}$$

where $i$ denotes tour $i$, $K_i$ is the number of trips in tour $i$, $J$ represents the non-driving choice set, and $\frac{1}{\mu}$ is the scale factor between nests. $V_{ijk}$ is the utility of mode $j$ of trip $k$ in tour $i$.

With respect to the utility function of each mode, the main attributes we consider are in-vehicle travel time and travel cost. The utility functions of the upper level alternatives are shown in Eq. (3.2a) (driving) and (3.2b) (non-driving). Eq. (3.3a) shows the utility functions of the lower

level non-driving modes except for public transit; Eq. (3.3b) shows the function for public transit. The alternative specific constant for carpool is set to zero, i.e. $\beta_{1,C} = 0$.

$$V_{driving,i} = \sum_{k=1}^{K_i} \left( \beta_{driving,C} + \frac{1}{\mu} \times \beta_{cost} \times Cost_{i,k,driving} \right) \tag{3.2a}$$

$$V_{non-driving,i} = E[V_{N_2,i}] \tag{3.2b}$$

$$V_{j,i,k} = \beta_{j,C} + \beta_{cost} \times Cost_{i,k,j} + \beta_{time,j} \times Time_{i,k,j}, \qquad j \in J \backslash \{1,2\} \tag{3.3a}$$

$$V_{2,i,k} = \beta_{2,C} + \beta_{cost} \times Cost_{i,k,2} + \beta_{time,2} \times (Time_{i,k,2} - Time_{i,k,driving})$$
$$+ \beta_{AT} \times AT_{i,k} + \beta_{ET} \times ET_{i,k} + \beta_{WT} \times WT_{i,k} + \beta_f \times f_{i,k} \tag{3.3b}$$

$\beta_{driving,C}$ is the alternative specific constant of driving and $Cost_{i,k,driving}$ is the cost of driving in tour $i$. For all the cost attributes, we use the same coefficient in the non-driving nest $N_2$ because people have the same perception of monetary cost. The $\frac{1}{\mu}$ is the scale factor between nests. In Eq. (3.3), $Cost_{i,k,j}$ is the $j$ for trip $k$ in tour $i$, $Time_{i,k,j}$ is the in-vehicle travel time (hr) of $j$ for trip $k$ in tour $i$. $WT_{i,k}$ denotes the wait time (hr) during transfer, $AT_{i,k}$ for transit access time (hr), $ET_{i,k}$ for transit egress time (hr), $f_{i,k}$ is a binary variable representing whether (1) or not (0) there is at least one transfer during the trip . For the transit utility function, we subtract the in-vehicle travel time of driving from in-vehicle travel time of transit for each trip to incorporate the in-vehicle travel time in the same level.

The model is applied to two different population segments: Manhattan and Non-Manhattan. People's travel patterns are different in Manhattan than outside Manhattan due to different built environments (transit accessibility, parking space, etc.). If the origin or destination of any trip in one tour is inside Manhattan, the whole tour is assigned to the Manhattan segment.

### 3.3.2 Estimation results

The travel cost for driving is comprised of parking cost and toll cost reported by 2010/2011 RHTS. For trips that have no response, the average parking and toll cost is assumed for the individual: $4.94 for each Manhattan-related trip and $1.37 for each Non-Manhattan-related trip. The cost of transit is $2.75 per trip. Taxi cost is calculated according to the standard metered fare from NYC Taxi and Limousine Commission (TLC) plus 8.875% tax and 20% tips (TLC, 2018). We also considered the wait times for taxi, assuming wait times for taxi are 3 minutes in Manhattan

and 5 minutes outside Manhattan. We added the wait times as the equivalent monetary cost to the travel cost of taxi. Carpool cost is assumed to be half that of taxi. There is no cost for bike and walking.

All the estimations are run in Python Biogeme version 2.6a on a MacBook Pro with 2.7 GHz Intel Core i5, 8GB memory. The results of both segments are presented in Table 4.

**Table 4. Estimation results of nested logit model for both segments**

| Manhattan segment | Variable number | Variable name | Coefficient estimate | Standard error | t statistic |
|---|---|---|---|---|---|
| | 1 | Auto constant | -2.15 | 0.10 | -22.53 *** |
| | 2 | Transit constant | 3.14 | 0.10 | 30.42 *** |
| | 3 | Taxi constant | 1.06 | 0.11 | 9.53 *** |
| | 4 | Bike constant | 0.44 | 0.13 | 3.54 *** |
| | 5 | Walk constant | 5.74 | 0.11 | 54.64 *** |
| | 6 | Travel cost ($) | -0.06 | 0.01 | -13.37 *** |
| | 7 | Carpool travel time (h) | 0.60 | 0.13 | 4.50 *** |
| | 8 | Transit travel time(h) | -1.74 | 0.28 | -6.18 *** |
| | 9 | Bike travel time(h) | -4.31 | 0.36 | -11.84 *** |
| | 10 | Walk travel time(h) | -5.70 | 0.14 | -39.50 *** |
| | 11 | Transit access time (h) | -2.71 | 0.46 | -5.88 *** |
| | 12 | Transit egress time(h) | -2.63 | 0.48 | -5.53 *** |
| | 13 | Transit transfer time(h) | -3.08 | 0.73 | -4.25 *** |
| | 14 | Transit transfer | -0.03 | 0.07 | -0.46 |
| | 15 | 1/mu | 0.03 | 0.01 | 3.23 * |

*, **, and *** indicate statistical significance at the 0.05, 0.01, 0.001 levels, respectively.

**Summary statistics**

upper level    Number of observations = 6935

Initial log likelihood = - 4806.976

Final log likelihood = -1944.573

Mcfadden Rho-square = 0.595

lower level    Number of observations = 13769

Initial log likelihood = -21217.510

| Non-Manhattan segment | Variable number | Variable name | Coefficient estimate | Standard error | t statistic |
|---|---|---|---|---|---|
| | | Final log likelihood = -7040.113 | | | |
| | | Mcfadden Rho-square = 0.668 | | | |
| | 1 | Auto constant | -0.48 | 0.05 | -10.28 *** |
| | 2 | Transit constant | 0.93 | 0.07 | 12.90 *** |
| | 3 | Taxi constant | -1.80 | 0.12 | -15.35 *** |
| | 4 | Bike constant | -1.35 | 0.11 | -12.13 *** |
| | 5 | Walk constant | 3.50 | 0.07 | 53.29 *** |
| | 6 | Travel cost ($) | -0.06 | 0.01 | -7.32 *** |
| | 7 | Carpool travel time (h) | 0.36 | 0.11 | 3.28 *** |
| | 8 | Transit travel time(h) | 0.00 | NA | NA |
| | 9 | Bike travel time(h) | -5.69 | 0.62 | -9.20 *** |
| | 10 | Walk travel time(h) | -5.06 | 0.13 | -38.54 *** |
| | 11 | Transit access time (h) | -1.71 | 0.34 | -5.11 *** |
| | 12 | Transit egress time(h) | -1.70 | 0.32 | -5.30 *** |
| | 13 | Transit transfer time(h) | -1.36 | 0.58 | -2.35 ** |
| | 14 | Transit transfer | -0.07 | 0.07 | -1.01 |
| | 15 | 1/mu | 0.11 | 0.01 | 8.91 *** |

*, **, and *** indicate statistical significance at the 0.05, 0.01, 0.001 levels, respectively.

**Summary statistics**

upper level   Number of observations = 8769

Initial log likelihood = -6078.208

Final log likelihood = -5298.416

Mcfadden Rho-square = 0.128

lower level   Number of observations = 10975

Initial log likelihood = -16503.397

Final log likelihood = -7851.371

Mcfadden Rho-square = 0.524

We calculated the value of time (VOT) in Manhattan segment by computing $\frac{\beta_{t,transit}}{\beta_{cost}} = \$29/h$. This value is higher than the \$22.87/hr reported in Lam and Small (2001), which makes

C2 SMART
CONNECTED CITIES WITH
SMART TRANSPORTATION

sense when considering inflation and higher cost of living in Manhattan. The VOT for non-Manhattan is not reported since it is not statistically significant.

### 3.3.3 Smartphone ownership model and mode choice update

Since the 2010/2011 RHTS didn't include choices of FHV and Citi Bike, we need to update our model to incorporate these two choices for our 2016 baseline model. Considering the choice of these two modes is highly correlated to the ownership of smartphone, we estimated a smartphone ownership model for NYC first.

The data comes from ACS household and person sample records (U.S. Census Bureau, 2016). Revealed preference data for smartphones is only available in household records, so we use single-person household records and match them to person records to obtain personal attributes. To be consistent with the data available from RHTS, the person's age, income and work status are selected as attributes. All the attributes are categorical and have the same classifications as in RHTS. The final estimated utility function specification for each individual $n$ choosing to own a smartphone is shown in Eq. (3.4) relative to $V_{no,n} = 0$.

$$V_{yes,n} = C_{yes} + \beta_{inc_1} \times inc_{1,n} + \beta_{inc_3} \times inc_{3,n} + \beta_{inc_4} \times inc_{4,n} \qquad (3.4)$$
$$+ \beta_{age_{56}} \times age_{56,n} + \beta_{age_7} \times age_{7,n} + \beta_{work} \times work_n$$

where $C_{yes}$ is an alternative-specific constant of having the smartphone, $inc_{i,n}$ is a binary variable for inclusion in annual income category $i$ (1: below \$30K, 3: \$75K-99.9K, 4: above \$100K) for person $n$, $age_{i,n}$ is a binary variable for inclusion in age category $i$ (56: 35-64, 7: older than 75) for person $n$, and $work_n$ indicates whether person $n$ works (1) or not (0).

We estimate the binary logit model using the open-source software PandasBiogeme (Bierlaire, 2018). The estimation was run on a desktop with Intel Xeon 3.5 GHz and 125 GB RAM. Table 5 shows the results of the estimated model. The coefficients of higher ages (group 5&6, and 7) are negative, which indicates that elderly people are less likely to own a smartphone. And people with higher income or with jobs are more likely to own a smartphone.

**Table 5. Results of coefficients of Smart Phone ownership model**

| Variable name | Coefficient estimate | Standard error | t statistic |
|---|---|---|---|
| Alt.Spec.Constant | 1.75 | 0.138 | 12.7 *** |
| Age groups 5 & 6 | -1.48 | 0.122 | -12.1 *** |
| Age group 7 | -2.63 | 0.126 | -20.8 *** |
| Income group 1 | -0.478 | 0.0679 | -7.04 *** |
| Income group 3 | 0.641 | 0.125 | 5.11 *** |
| Income group 4 | 0.789 | 0.113 | 6.96 *** |
| Work status | 1.08 | 0.0681 | 15.9 *** |

*, **, and *** indicate statistical significance at the 0.05, 0.01, 0.001 levels, respectively.

**Summary statistics**

Number of observations = 8030

Initial log likelihood = -5565.972

Final log likelihood = -3911.692

McFadden Rho-square = 0.297

We updated the model to incorporate new mobility services. According to the synthetic population in 2016, the total number of daily trips is 30.5M, excluding the FHV and Citi Bike trip counts. The total daily trips from 2010/2011 RHTS is 23.8M. The total daily trips increased by 28.33% from 2011 to 2016, so we expanded the trips in 2011 by this factor to fit for 2016.

The probability of owning a smartphone obtained from the previous model was regarded as the availability of FHV. The probability of choosing FHV is shown in Eq. (3.5). $P_{i,k}(FHV)$ represents the probability of choosing FHV for trip $k$ in tour $i$, $V_{6,i,k}$ is identical to that of choosing taxi except for the alternative specific constant which needs to be estimated, i.e. $V_{6,i,k} = \beta_{6,C} + \beta_{cost} \times Cost_{i,k,6} + \beta_{time,3} \times Time_{i,k,6}$ , and $P_{SM,i}(yes)$ is the probability of owning a smartphone in tour $i$. The $Time_{i,k,6}$ for FHV is assumed to be 80% that of taxi, resulting in 2.4 minutes in Manhattan and 4 minutes outside Manhattan.

$$P_{i,k}(FHV) = P_{i,k}(FHV|N_2) \times P_i(N_2) \times P_{SM,i}(yes)$$
$$= \frac{e^{V_{6,i,k}}}{\sum_j^{J^*}(e^{V_{j,i,k}})} \times \frac{E[V_{N_2,i}]}{E[V_{N_2,i}] + e^{V_{N_1,i}}} \times \frac{e^{V_{yes}}}{e^{V_{yes}} + 1} \qquad (3.5)$$

The presence of FHV also impacts other modes because it affects the choice set. The probability of choosing each mode except FHV is calculated with Eq. (3.6). $P_{i,k}(m)$ denotes the probability of choosing mode $m$ (excluding FHV) for trip $k$ in tour $i$. Since the probability of owning a smartphone is interpreted as the availability of FHV, the probability of choosing each mode is calculated as the expected probability conditional on owning a smartphone. $P_{i,k}(m|N_2) \times P_i(N_2)$ includes FHV in the choice set whereas $P'_{i,k}(j|N_2) \times P'_i(N_2)$ does not.

$$P_{i,k}(m) = P_{i,k}(m|N_2) \times P_i(N_2) \times P_{SM,i}(yes)$$
$$+ P'_{i,k}(j|N_2) \times P'_i(N_2) \times (1 - P_{SM,i}(yes))$$

$$= \frac{e^{V_{m,i,k}}}{\sum_j^{J^*}(e^{V_{j,i,k}})} \times \frac{E[V_{N_2,i}]}{E[V_{N_2,i}] + e^{V_{N_1,i}}} \times \frac{e^{V_{yes}}}{e^{V_{yes}} + 1} \tag{3.6}$$

$$+ \frac{e^{V_{m,i,k}}}{\sum_{j\neq 6}^{J^*}(e^{V_{j,i,k}})} \times \frac{E[V_{N_2,i}]_{j\neq 6}}{E[V_{N_2,i}]_{j\neq 6} + e^{V_{N_1,i}}} \times \frac{1}{e^{V_{yes}} + 1}, \forall m \in J^* \text{ and } m \neq 6$$

The utility of the Citi Bike choice is shown in Eq. (3.7).

$$V_{i,k,7} = \beta_{7,C} + \beta_{cost} * Cost_{i,k,7} + \beta_{time,4} * Time_{i,k,7} + \beta_{smartphone} * P_{SM,i}(yes) \tag{3.7}$$

In summary, we need to estimate the following parameters for the two emerging mobility modes: $\beta_{6,C}, \beta_{smartphone}, \beta_{7,C}$, for two different segments, Manhattan and non-Manhattan (six parameters in total).

Estimation of the three parameters is done using the aggregation of the choices from the two market segments in 2016 compared to observed trips generated per zone, using nonlinear least squares regression (NLSR). The objective of the NLSR estimation is shown in Eq. (3.8).

$$\min z_{\beta_{6,C},\beta_{smartphone},\beta_{7,C}}$$
$$= \sum_{i=1}^{N} \left[ \left(Trip_{pre,i,FHV} - Trip_{obs,i,FHV}\right)^2 + \left(Trip_{pre,i,CB} - Trip_{obs,i,CB}\right)^2 \right] \tag{3.8}$$

where $Trip_{pre,i,FHV} = Trip_{pre,i,FHV,Manhattan} + Trip_{pre,i,FHV,nonManhattan}$, and $N = \{1,2,\dots,1622\}$ is the set of TAZs in NYC. The NLSR is run in MATLAB 2016a on a desktop with Intel® Core™ i7-6700 CPU @ 3.40 GHZ, 16 GB RAM. The calculation time is 531 seconds.

A bootstrapping method was adopted to measure the statistical significance of the estimated coefficients. The coefficient set generated by bootstrapping (Chernick and LaBudde, 2014) has

50 bootstrap samples for each coefficient. The estimated coefficients from the NLSR and the statistical significance tests are shown in Table 6. The approximate t-stats based on bootstrapping suggest the coefficients are statistically significant.

**Table 6. Estimated parameters and confidence intervals for FHV and Citi Bike**

| Segment | No. | Variable name | Estimated value | Bootstrap | | | t-stat |
| | | | | Lower bound | Upper bound | Standard Error | |
|---------|-----|---------------|-----------------|-------------|-------------|----------------|--------|
| Manhattan | 1 | Citi Bike Constant | -0.35 | -0.53 | -0.11 | 0.09 | -3.89*** |
| | 2 | FHV Constant | 0.80 | 0.69 | 0.92 | 0.06 | 13.33*** |
| | 3 | Smartphone | -0.34 | -0.67 | -0.06 | 0.10 | -3.40*** |
| Non-Manhattan | 4 | Citi Bike Constant | -1.91 | -2.64 | -1.67 | 0.20 | -9.55*** |
| | 5 | FHV Constant | -3.46 | -3.89 | -2.74 | 0.21 | -16.48*** |
| | 6 | Smartphone | -1.51 | -2.11 | -1.34 | 0.16 | -9.44*** |
| Num. Obs. | 1622 | | | | | | |
| RMSE (%CV) | FHV: 401.83 trips/zone (154% NYC, 51% Manhattan) | | | Citi Bike: 59.80 trips/zone (54%) | | | |
| *, **, and *** indicate statistical significance at the 0.05, 0.01, 0.001 levels, respectively. | | | | | | | |

To validate the model, we compared the aggregated mode share from the synthetic population to the 2017 Citywide Mobility Survey (CMS) from NYC DOT. The results are presented in Figure 12. Comparing to the mode share of 2011 RHTS, the prediction of synthetic population is closer to the 2017 CMS.
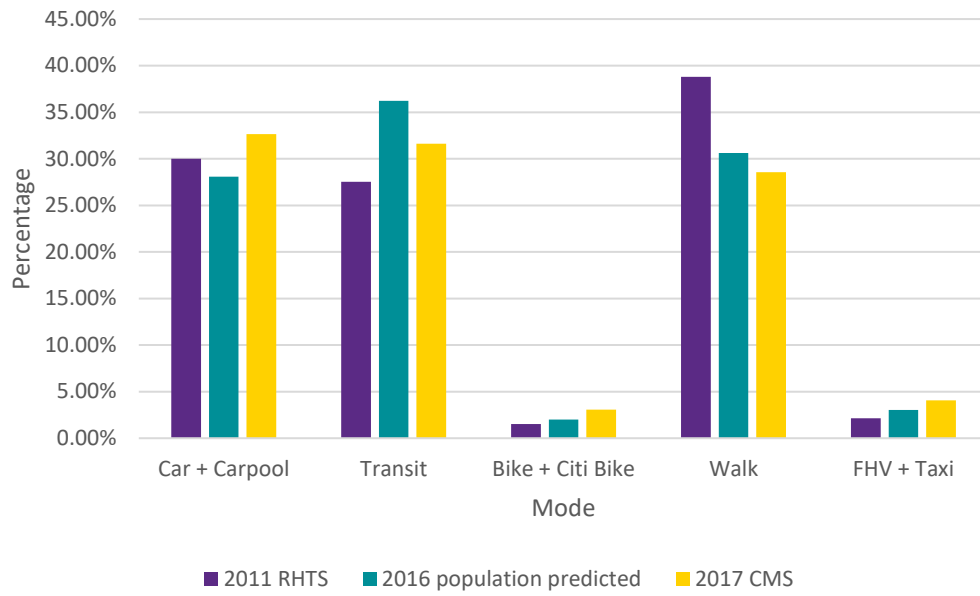
**Figure 12. Aggregated mode share of 2011 RHTS, synthetic population and 2017 CMS.**

## Section 4: Baseline model calibration

As introduced in Section 2, MATSim uses a queue model to simulate traffic dynamics. We calibrate the road network in the baseline model to capture factors not considered: e.g. arterial traffic systems, non-resident (tourist) trips, truck deliveries. The synthetic population's mode choice model also needs to be adjusted to fit the MNL-oriented model structure from the nested logit model.

### 4.1 Data preparation

#### 4.1.1 Modal networks

The Modal networks consists of a road network transformed from Open Street Map (OSM) data and a transit network generated from GTFS data. The transformation of road network is conducted via the open-source Java-based network edit tool JOSM (JOSM, 2018). The OSM data is extracted in November 2018. The road network is shown in Figure 13. We classified the links of road network to two categories: Arterial link and Freeway link. If the free flow speed of a link is above 33.33 m/s (about 75 mph), it belongs to a Freeway link, otherwise it is an Arterial link.

The transit network is generated from GTFS data (MTA, 2018) in September 2016. The stop locations, operation schedules and timetables are the same as in the historical data. Vehicle capacities are also calibrated. We combined the transit network with the road network using MATSim extension "pt2matsim". The combined modal network is presented in Figure 14. The routes of transit lines are artificially generated according to the distances between stations and operation timetables, instead of searching in the road network. As a result, the transit assignment is simulated on dedicated links.
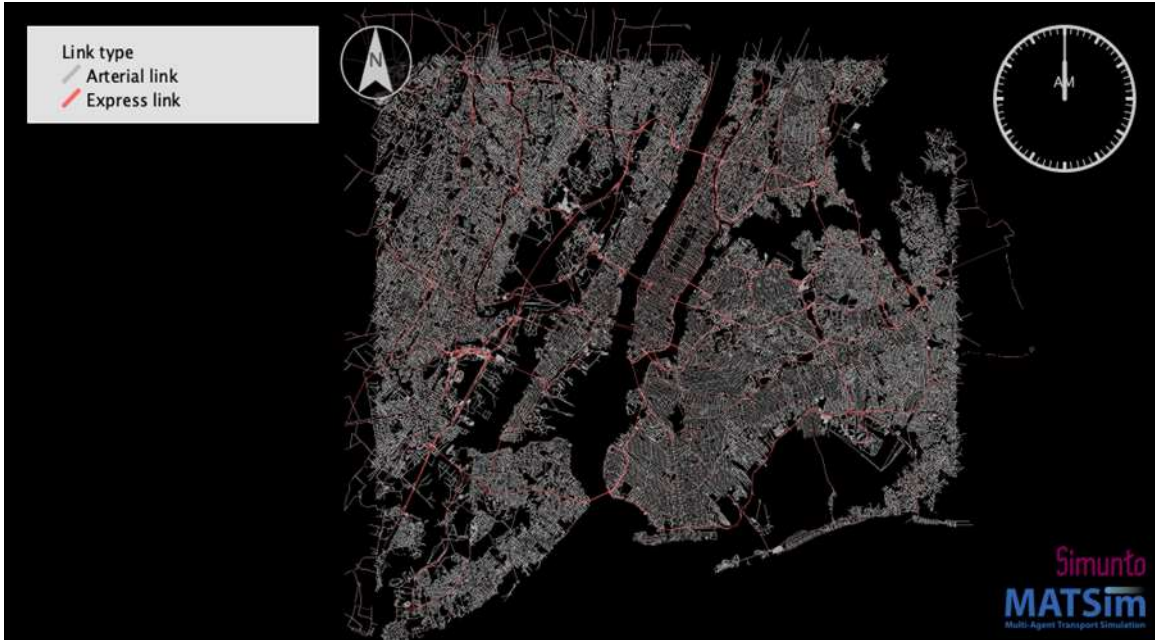
**Figure 13. Road network from OSM data.**



**Figure 14. Modal network of NYC.**

## 4.1.2 Extended travel demand

In Section 3, we developed the synthetic population of NYC with personal information, travel agendas and mode choices. However, this population only incorporates city residents. Those who live outside the city but travel to NYC are not included, which would lead to less volumes in some areas. Therefore, we generated a subpopulation of those non-residential travelers to compensate for the missing volumes. The subpopulation is duplicated from the 2011 RHTS, keeping the agendas the same. The modes are aggregated to walking, driving and transit. For the trips cross the boundary of the city, the origin/destination of inside/outside trips will be switched to the nearest gateway by modes. The locations of all the gateways are shown in Figure 15. In the end, a 1.18M population was added to the simulation with 3.04M trips.



**Figure 15. Gateway locations around the city.**

## 4.1.3 Activity and travel parameters in MATSim

In MATSim, each agent has multiple plans in a day and selects one to execute among them. To evaluate the plans, a score is calculated for each plan, which is similar to the mode utility in

the mode choice model but incorporates the additional utility (score) of activities (Nagel et al., 2016). The basic function of calculating the plan score is shown in Eq. (4.1).

$$S_{plan} = \sum_{q=0}^{N-1} S_{act,q} + \sum_{q=0}^{N-1} S_{trav,mode(q)} \tag{4.1}$$

where $N$ is the number of activities in the plan, $S_{act,q}$ refers to the score of activity $q$ and $S_{trav,mode(q)}$ represents the score of trip after activity $q$ by $mode(q)$. The last activity is combined with the first one to have the same number of activities and trips. The score functions are shown in Eqs. (4.2a) – (4.2d).

$$S_{dur,q} = \beta_{dur} * t_{typ,q} * \ln{(t_{dur,q}/t_{0,q})} \tag{4.2a}$$

$$S_{wait,q} = \beta_{wait} * t_{wait,q} \tag{4.2b}$$

$$S_{late\ arr,q} = \begin{cases} \beta_{late\ arr} * (t_{start,q} - t_{latest\ arr,q}), if\ t_{start,q} > t_{latest\ arr,q} \\ 0, otherwise \end{cases} \tag{4.2c}$$

$$S_{early\ dep,q} = \begin{cases} \beta_{early\ dep} * (t_{earliest\ dep,q} - t_{end,q}), if\ t_{earliest\ dep,q} > t_{end,q} \\ 0, otherwise \end{cases} \tag{4.2d}$$

$$S_{short\ dur,q} = \begin{cases} \beta_{short\ dur} * (t_{short\ dur,q} - t_{dur,q}), if\ t_{short\ dur,q} > t_{dur,q} \\ 0, otherwise \end{cases} \tag{4.2e}$$

where $t_{typ,q}$ is the typical duration of activity $q$, $t_{dur,q}$ is the actual duration of activity $q$, $t_{0,q}$ is the duration when the utility of activity $q$ starts to be positive. $t_{0,q}$ is set to $t_{typ,q} \times \exp{(-10h/t_{typ,q})}$ according to Rieser et al. (2014). We have five activity types defined in MATSim: Home, Work, School, University and Secondary. MATSim defines the maximum durations for the whole population by activity type: we set the maximum durations of the activities as 8h, 8h, 8h, 1h and 1h correspondingly. $t_{wait,q}$ is the wait time before activity $q$ starts, $t_{start,q}$ is the actual start time of activity $q$, $t_{latest\ arr,q}$ is the latest start time of activity $q$ without penalty, $t_{end,q}$ is the actual end time of activity $q$, $t_{earliest\ dep,q}$ is the earliest possible leaving time of activity $q$, $t_{short\ dur,q}$

C2SMART
CONNECTED CITIES WITH
SMART TRANSPORTATION

is the shortest possible duration of activity $q$. Eq. (4.2a) defines the score of performing an activity, which is usually positive. Eq. (4.2b) represents the wait penalty. Eq. (4.2c) is the penalty of late arrival, Eq. (4.2d) is the penalty of early departure, and Eq. (4.2e) denotes the penalty for a "too short" activity. $\beta_{wait}$, $\beta_{early\ dep}$, $\beta_{short\ dur}$ are recommended to be 0 according to Nagel et al. (2016), if no data is available to determine those parameters. $\beta_{dur}$ is set to be the same as the positive value of the parameter for travel time of driving alone, and the $\beta_{late\ arr}$ is determined relative to the parameter of travel time of driving alone according to Small (1982). Small (1982) proposed a scheduling model for work trips and the results indicated that the parameter of schedule delay is about 2.39 times of travel time. We use this to estimate a $\beta_{late\ arr} = -4.19$. The parameters used to calculate the activity score in MATSim-NYC are presented in Table 7. Since $\beta_{dur}$ is assumed in order to have agents try to maximize their durations, we make sure to omit the duration attribute from the score calculations when determining consumer surplus (i.e. the consumer surplus measure reported in our results captures travel disutilities and schedule delays, not activity participation utility).

**Table 7. Parameters for activity score in MATSim**

| $\beta_{dur}$ | $\beta_{wait}$ | $\beta_{late\ arr}$ | $\beta_{early\ dep}$ | $\beta_{short\ dur}$ |
|---|---|---|---|---|
| 1.75 | 0 | -4.19 | 0 | 0 |

Since the default MATSim only supports mode choice with the Multinomial Logit (MNL) model, we adjusted the tour-based nested logit model into a trip-based MNL model as shown in Eqs. (4.3a) – (4.3c). The smartphone ownership model and the availability of Citi Bike are ignored as well in MATSim.

$$V_{driving,k} = \beta_{driving,C} * \mu + \beta_{cost} \times Cost_{k,driving} \tag{4.3a}$$

$$V_{j,k} = \beta_{j,C} + \beta_{cost} \times Cost_{k,j} + \beta_{time,j} \times Time_{k,j}, \qquad j \in J \backslash \{1,2\} \tag{4.3b}$$

$$V_{2,k} = \beta_{2,C} + \beta_{cost} \times Cost_{k,2} + \beta_{time,2} \times (Time_{k,2} - Time_{k,driving}) + \beta_{AT} \times AT_k$$
$$+ \beta_{ET} \times ET_k + \beta_{WT} \times WT_k + \beta_f \times f_k \tag{4.3c}$$

where all the notations are defined as before, only without the subscription $i$ for tour. The equivalent parameters used for the travel score in MATSim-NYC are shown in Table 8. The travel

time parameter of car was regarded as the reference and the travel time parameters of of the other modes were adjusted accordingly (including the parameters of Access Time, Egress Time, and Transfer Time).

**Table 8. Parameters for travel score of both Manhattan and Non-Manhattan segments**

| Manhattan | | car | carpool | transit | taxi | bike | walk | Citi Bike | FHV |
|---|---|---|---|---|---|---|---|---|---|
| Constant | | -0.06 | 0.00 | 2.95 | 1.06 | 0.44 | 5.73 | -0.37 | 0.79 |
| Travel Time | | 0 | 2.35 | 0.00 | 1.75 | -2.55 | -3.94 | -2.55 | 1.75 |
| Cost | | -0.06 | | | | | | | |
| transit | Access Time | -0.96 | | | | | | | |
| | Egress Time | -0.86 | | | | | | | |
| | Transfer Time | -1.46 | | | | | | | |
| Non-Manhattan | | car | carpool | transit | taxi | bike | walk | Citi Bike | FHV |
| Constant | | -0.05 | 0.00 | 0.76 | -1.81 | -1.35 | 3.49 | -2.04 | -3.38 |
| time | | 0.00 | 0.36 | 0.00 | 0.00 | -5.64 | -5.05 | -5.64 | 0.00 |
| cost | | 0 | | | | | | | |
| transit | Access Time | -1.71 | | | | | | | |
| | Egress Time | -1.67 | | | | | | | |
| | Transfer Time | -1.61 | | | | | | | |

## 4.2 Network calibration

### 4.2.1 Overview of MATSim Traffic Flow Model

MATSim adopted a computationally efficient queue-based approach to simulate traffic flow (Horni et al., 2016). Dobler and Axhausen (2011) gave an overview of the parallel queue-based traffic simulation implemented in MATSim. In the queue-based model, the flow capacity, storage capacity, and free flow speed link travel time are taken into consideration (Agarwal et al., 2015). First, the flow capacity defines the number of vehicles leaving a link per time step. Second, the storage capacity refers to the number of vehicles fitting onto a network link, which is calculated by the length of link divided by the equivalent length of vehicle and multiplied number of lanes. However, this constraint can be relaxed during simulation for some overcrowded links to maintain a minimal flow (Horni and Nagel, 2016). The configuration parameter in MATSim "stuck time" defines the threshold for a vehicle to stay stationary. The default value of stuck time is 10,

i.e., a stationary vehicle is moved forward after 10 time steps. Lastly, as the name indicates, the free flow speed link travel time is calculated by the link length over link free flow speed.

The queue-based model regards a network link (i.e. a road segment) as a queue. When a vehicle is entering the link, it is added to the tail of the waiting queue at the start of the link. The vehicle can enter the link until it becomes the head of the queue, the downstream link allows entering and the link flow capacity is not exceeded. Once the vehicle entered a link, the travel time on that link will be the free flow speed link travel time. The Fundamental Diagrams (FDs) of the queue-based model are presented in Figure 16.
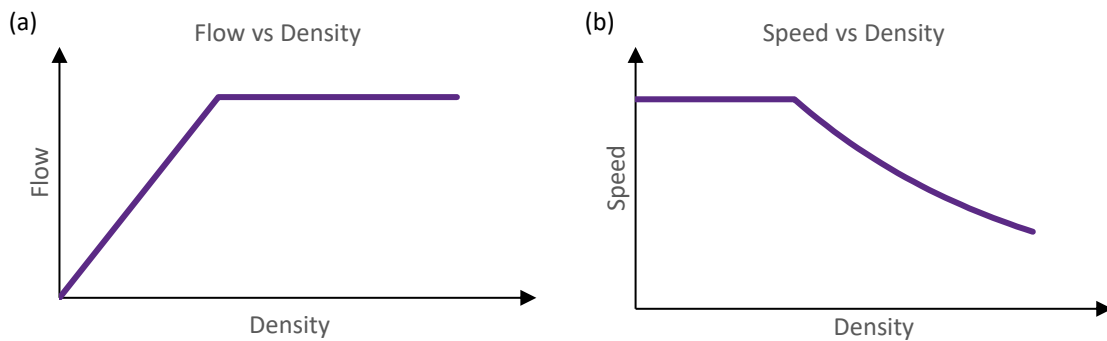


**Figure 16. FDs of MATSim queue-based model (a) Flow vs Density and (b) Speed vs Density.**

The queue-based model ignores the intra-link interactions to improve the computational efficiency. When a link is saturated, the flow stays the same in MATSim as long as the downstream link is open, while in the real world, the flow goes down as the density increases. This assumes that the MATSim equilibrium operates in a steady state where traffic would not be oversaturated. Speed, even though it goes down with density after the link is saturated, is still higher than the real speed because vehicles travel with free flow speed after entering a link. Improvements are made to address these limitations in Section 6.

### 4.2.2 Calibration framework

Since the storage capacity is always set large enough or relaxed by configuration, the link flow capacity and free flow speed are the major attributes that influence the traffic flow simulation in MATSim. In the MATSim-NYC model, the road network is transformed from OSM data which has imprecise link flow capacities and free flow speeds and therefore cannot represent the real road network. Other factors (e.g. arterial traffic system, non-resident (tourist) trips, truck deliveries, etc.) that affect the link flow capacity and free flow speed are not incorporated due to limitations of the data. The road network attributes (link flow capacity and free flow speed) need to be calibrated to make the simulation model more realistic.

We defined two sets of parameters for those two major network attributes. Based on the queue-based model, vehicles travel with unsaturated flow speed when entering a link. Therefore, the link unsaturated flow speed parameters are calibrated first according to the INRIX speed data and then implemented in the road network. The link capacity factors are perturbated iteratively to find the equilibrium of the calibrated link capacity and unsaturated flow speed, which leads to a closer volume distribution compared to the real traffic count. The overview of the process is shown in Figure 17.
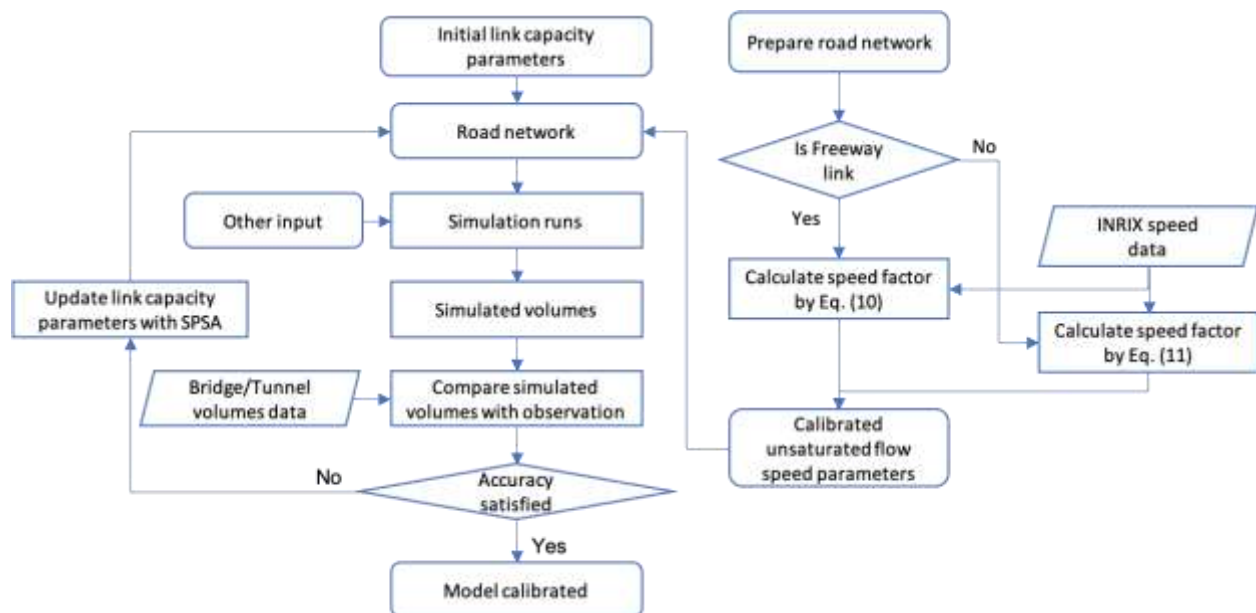


**Figure 17. The framework of calibration process.**

### 4.2.3 Reference data

The 2016 bridges/tunnels volumes data (NYCDOT,2016) and INRIX speed data in September, 2016, from DOT were used as the calibration reference data. The volumes data contains hourly average traffic counts of 59 bridges/tunnels around the city on a typical weekday. The speed data includes observed 5-minute speeds for 6,996 link segments across the city.

We selected 19 facilities from the volumes data to calibrate the road capacities, as shown in Table 9. A screenline along East River was defined, as red curves shown in Figure 18, which consists of Queensboro Bridge, Williamsburg Bridge, Queens Midtown Tunnel, Manhattan Bridge, Brooklyn Bridge, and Hugh Carey Tunnel. The Hudson River crossings are not considered since most of the trips are made by non-residents which are not sensitive to the calibration of the road network.

**Table 9. List of traffic count facilities**

| ID | Facility | ID | Facility | ID | Facility |
|---|---|---|---|---|---|
| 1 | Brooklyn Bridge | 8 | Washington Bridge | 15 | Verrazzano-Narrows Bridge |
| 2 | Ed Koch Queensboro Bridge | 9 | Willis Avenue Bridge | 16 | George Washington Bridge |
| 3 | Williamsburg Bridge | 10 | 145th Street Bridge | 17 | Holland Tunnel |
| 4 | Alexander Hamilton Bridge | 11 | Hugh L. Carey Tunnel | 18 | Lincoln Tunnel |
| 5 | Macombs Dam Bridge | 12 | Queens-Midtown Tunnel | 19 | Manhattan Bridge |
| 6 | Madison Avenue Bridge | 13 | Robert F. Kennedy Memorial Bridge Manhattan Plaza | | |
| 7 | University Heights Bridge | 14 | Robert F. Kennedy Memorial Bridge Bronx Plaza | | |

**Figure 18. Select facilities for link capacity calibration and East River screenline.**

For the speed calibration, we took the average hourly speed on weekdays of September, 2016, as reference. Figure 19 presents the distribution of average observed speed at 12 AM.



**Figure 19. Distribution of average hourly speed at 12 AM from INRIX data.**

### 4.2.4 Link unsaturated flow speed calibration

The default link free flow speed in MATSim is fixed across a day, while the speed from INRIX data varies with time. We adopted a time-variant network to capture the variation of link free flow speed in our simulation. Six time periods are defined for one day: 6 - 9 AM, 9 AM - 12 PM, 12 - 3 PM, 3 - 6 PM, 6 - 9PM and 9 PM - 6 AM. Different speed factors were applied to links according to link types (defined in Section 4.1.1) and time. Denote $L = \{1,2\}$, where 1 is freeway and 2 is arterial, and $T = \{1,2,3,4,5,6\}$ refers to six time periods correspondingly.

First, the average speed data from INRIX were aggregated by link type and time period (Table 10). We can calculate the link speed factors of each freeway link as Eq. (4.4).

$$f_{1,t}^{s} v_1^0 = v_{1,t}^{ob}, t \in T \qquad (4.4)$$

where $v_{1,t}^{ob}$ refers to the average observed speed for the freeway link in time period $t$, and $v_1^0$ represents the default free flow speed for the freeway link.

**Table 10. Average observed speed in each time period for Freeway and Arterial links (mph)**

|          | 6AM-9AM | 9AM-12PM | 12PM-3PM | 3PM-6PM | 6PM-9PM | 9PM-12AM |
|----------|---------|----------|----------|---------|---------|----------|
| Freeway  | 36.88   | 37.93    | 37.61    | 33.05   | 36.25   | 42.41    |
| Arterial | 14.10   | 13.42    | 13.11    | 12.80   | 13.91   | 15.34    |

For Arterial links, further adjustments are needed due to high variation in free flow speed. A set of sub-categories $J = \{1,2,3\}$ is used to represent arterial links with free flow speeds 22.2 m/s, 15.0 m/s and 8.3m/s, respectively. To adjust the link speed as close to observed speed as possible, we applied different link speed factors to corresponding sub-categories of arterial links using Eq. (4.5).

$$f_{2,t,j}^{s} v_{2,j}^0 = v_{2,t}^{ob}, t \in T, j \in J \qquad (4.5)$$

where $v_{2,j}^0$ is the default link free speed for link sub-category $j$.

### 4.2.3 Link capacity calibration

After the free flow speeds are adjusted to accommodate time-varying conditions like non-resident traffic and signal control, the next step is the capacity calibration. Based on the time variant network feature of MATSim, a link behaves according to Eq. (4.6).

$$C_{l,t}^{sim} = C_l^0 f_{l,t}^c \tag{4.6}$$

where $C_{l,t}^{sim}$ is the link flow capacity in simulation for facility type $l \in L$ in time period $t \in T$, $C_l^0$ is the default link capacity for facility type $l \in L$ from OSM, and $f_{l,t}^c$ is a factor to adjust the capacity for a given facility type $l \in L$ in time period $t \in T$. The storage capacities are unchanged from the default values (average vehicle length set to 7.5 m). The flow capacities are used in a cellular automata model to propagate traffic within the road network to output location volumes by time of day within one day. The simulation then proceeds through multiple days with each subsequent day updating the travel choices of the population and the cellular automata model updates the system performance based on the propagation of the new day's traffic. The resulting output of $n$ days of simulation is denoted as $\Omega_n$, i.e. $\left(\{V_{i,t}^{sim}\}\right) = \Omega_n(\theta, I; f^s)$ for location $i$ at time period $t$. In our model there are 12 (2 types, 6 periods) capacity parameters to be calibrated. The 19 locations in Table 9 are used for the calibration.

The objective is to minimize the simulation error with respect to the observed data (Yu and Fan, 2017). The loss function $L(\theta, I; f^s)$ is a response to a set of parameters and model input data $I$ given speed factors $f^s$. It is shown in Eq. (4.7). $\theta$ is a generic term representing the set of flow capacity factors $f_{l,t}^c$.

$$\min L(\theta, I; f^s) = \sum_{i \in N} \sum_{t \in T} \left|V_{i,t}^{ob} - \Omega(\theta, I; f^s)\right| / V_{i,t}^{ob} \tag{4.7}$$

where $V_{i,t}^{ob}$ and $V_{i,t}^{sim}$ are the average observed volumes and average simulated volumes of location $i$ in time period $t$.

To estimate the capacity parameters $\theta$ in Eq. (4.7), the approach of stochastic approximation (SA) is applied (Robbins and Monro, 1951). The SA approach is an iterative algorithm to update the parameter set. Let $\hat{\theta}_k$ denote the estimate for $\theta^*$ at the $k$th iteration. The standard form of

the update algorithm is shown in Eq. (4.8), where $g_k$ is the gradient and $a_k$ is a step size at the $k$th iteration.

$$\hat{\theta}_k = \hat{\theta}_{k-1} - a_{k-1} g_{k-1}(\hat{\theta}_{k-1}) \qquad (4.8)$$

The general idea of the SA algorithm is to mimic the gradient search method used in deterministic optimization problems, which requires a gradient of the loss function for the parameter update. However, for a traffic simulation model, the analytical form of the gradient of $\Omega(\theta, I; f^s)$ is not available for calculation. A numerical approximation of the gradient is obtained instead. With an approximated gradient, Equation (4.8) can be rewritten as Eq. (4.9).

$$\hat{\theta}_k = \hat{\theta}_{k-1} - a_{k-1} \hat{g}_{k-1}(\hat{\theta}_{k-1}) \qquad (4.9)$$

A well-known method for gradient approximation is the finite-difference (FD) method (Dennis and Schnabel, 1989). This method has two types, namely, one-sided and two-sided approximation. They are shown as:

$$\hat{g}_k(\hat{\theta}_k) = \begin{bmatrix} \dfrac{L(\hat{\theta}_k + c_k e_1) - L(\hat{\theta}_k)}{c_k} \\ \vdots \\ \dfrac{L(\hat{\theta}_k + c_k e_p) - L(\hat{\theta}_k)}{c_k} \end{bmatrix} \qquad (4.10)$$

$$\hat{g}_k(\hat{\theta}_k) = \begin{bmatrix} \dfrac{L(\hat{\theta}_k + c_k e_1) - L(\hat{\theta}_k - c_k e_1)}{2c_k} \\ \vdots \\ \dfrac{L(\hat{\theta}_k + c_k e_p) - L(\hat{\theta}_k - c_k e_p)}{2c_k} \end{bmatrix} \qquad (4.11)$$

where $e_i$ denotes a vector with a one in the $i$th place and zeros elsewhere. However, this method is not computationally efficient for problems with an increasing parameter size. For example, if the number of parameters is p, the one-sided approximation needed to calculate p+1 functions and the two-sided one needs 2p functions. The computational effort increases linearly with the number of parameters. To address this difficulty, the simultaneous perturbation stochastic approximation (SPSA) algorithm provides a good alternative to the FD method.

The SPSA method (Spall, 1988, 1998a, 1998b) requires only two measurements to approximate the gradient at each iteration regardless of the dimension of the parameters vector

$\theta$. This is achieved as all elements of the $\hat{\theta}_k$ vector are varied simultaneously, instead of calculating the measurements one by one for p+1 or 2p times like in the FD method. The formulation for SPSA algorithm is shown as:

$$\hat{g}_k(\hat{\theta}_k) = \begin{bmatrix} \dfrac{L(\hat{\theta}_k + c_k\Delta_k) - L(\hat{\theta}_k - c_k\Delta_k)}{2c_k\Delta_{k1}} \\ \vdots \\ \dfrac{L(\hat{\theta}_k + c_k\Delta_k) - L(\hat{\theta}_k - c_k\Delta_k)}{2c_k\Delta_{kp}} \end{bmatrix} = \dfrac{L(\hat{\theta}_k + c_k\Delta_k) - L(\hat{\theta}_k - c_k\Delta_k)}{2c_k} \begin{bmatrix} \Delta_{k1}^{-1} \\ \Delta_{k2}^{-1} \\ \vdots \\ \Delta_{kp}^{-1} \end{bmatrix} \qquad (4.12)$$

The approximation function for each parameter is the same except the perturbation term. This means the measurement of the loss function just needs to be calculated twice, $L(\hat{\theta}_k + c_k\Delta_k)$ and $L(\hat{\theta}_k - c_k\Delta_k)$. Compared with the FD method, this provides significant computational improvement for optimization analysis. More detailed discussion of SPSA algorithm can be found refer in Spall (1988, 1998a, 1998b). The capacity calibration algorithm is summarized in Figure 17. The SPSA method from Spall is shown in Algorithm 1.

**Algorithm 1: SPSA (source: Spall (1988, 1998a, 1998b))**

---

Input: initial vector of link capacity factors $\hat{\theta}_0$

---

0: Initialization

    Set $k = 1, \beta, \gamma, a, A, c$ as initial values.

1: Generation of simultaneous perturbation vectors

    Generate a $p$-dimension $\Delta_k$ by Monte Carlo. Each element of $\Delta_k$ is generated

    independently from a Bernoulli $\pm 1$ distribution with probability of ½.

    Calculate $a_k = \dfrac{a}{(k+A)^\beta}$ and $c_k = \dfrac{c}{k^\gamma}$.

2: Gradient approximation

    Calculate the gradient by Eq. (4.9).

3: Update $\hat{\theta}_k$ estimation

    Update $\hat{\theta}_k$ by Eq. (4.6).

Terminate the algorithm when loss function in Eq. (4.9) reached the threshold or the maximum iteration were reached, or set $k = k + 1$ and return step 1.

---

Output: final vector of link capacity factors $\hat{\theta}_k$

---

The SPSA method was implemented in Java and run with the MATSim-NYC model. The initial coefficients are $\beta = 0.602, \gamma = 0.101, a = 0.16, A = 3000, c = 0.05$. The initial value of the link flow capacity factor is 0.6. The upper bound and lower bound of link capacity factors are set as 0.8 and 0.3 to make sure the link capacities stay in a reasonable range. To save computation time for calibration, we ran only $n = 50$ days in MATSim for each iteration of the calibration.

## 4.3 Calibration Results

The calibration was running on a desktop with Intel(R) Xeon(R) CPU E5-2637 v4 @ 3.50GHz processors and 128GB RAM. We ran the calibration for 6 iterations until the simulated screenline volumes were observed to be close to the observed data. Each iteration took around 11 hours. The calibrated link capacity factors are presented in Table 11.

**Table 11. Calibrated link capacity factors for Freeway and Arterial links**

|  | 6AM-9AM | 9AM-12PM | 12PM-3PM | 3PM-6PM | 6PM-9PM | 9PM-12AM |
|---|---|---|---|---|---|---|
| Freeway | 0.61 | 0.69 | 0.51 | 0.63 | 0.55 | 0.68 |
| Arterial | 0.59 | 0.51 | 0.57 | 0.50 | 0.46 | 0.68 |
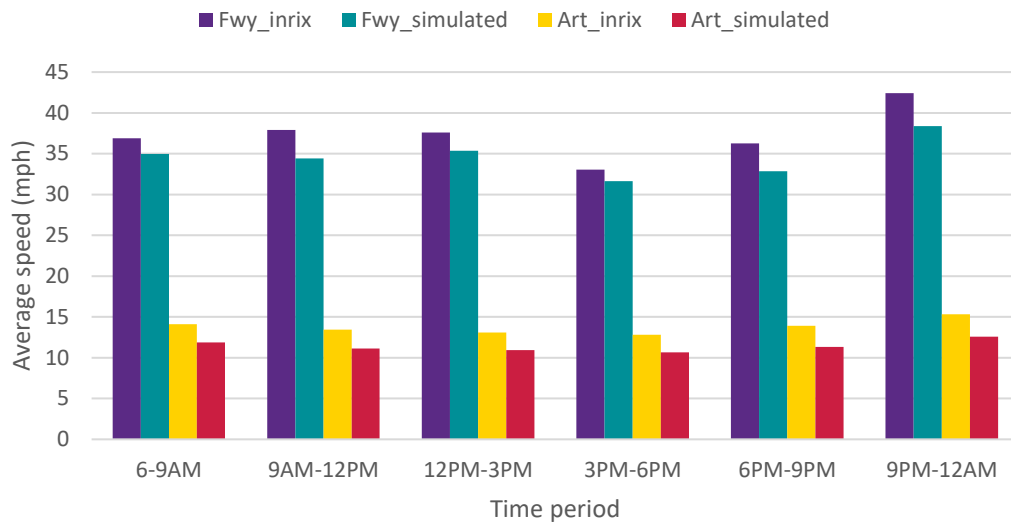
**Figure 20. Comparison of INRIX speed (observed) and simulated speed.**

As Figure 20 shows, the simulated average speed in each time period is close to the INRIX speed. For the Freeway links, the relative difference is 7.2% on average, with the highest of 9.5%. For the Arterial links, the relative difference is 17.1% on average, with the highest at 18.5%. The results of the Arterial links are worse because the default free flow speeds of the Arterial links vary more.
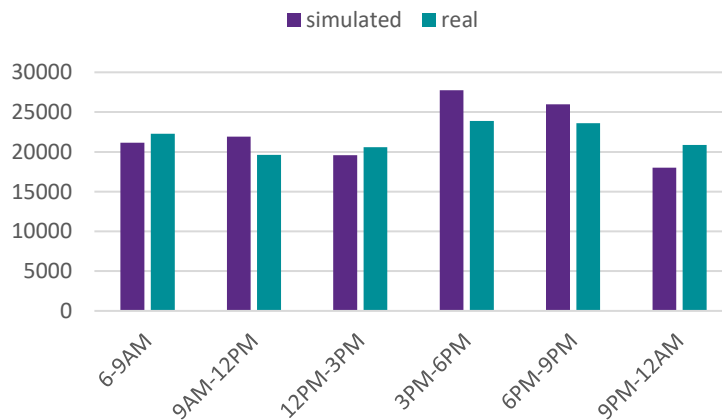


**Figure 21. Average simulated and real volume distribution of East River screenline across all time periods.**

The simulated volumes of the screenlines are also close to the real traffic count. For the East River screenline, the difference between the total daily simulated volumes and real volumes is only 2.6%. If we look at different time periods, the relative difference is 10.3% on average, with the highest at 16.3%.

We also compared the calibration results of East River screenline with the NYBPM 2010 update (Brinckerhoff, 2014). The results are presented in Table 12. The MATSim NYC model has the similar difference of East River screenline with NYBPM, which is 2.6% to -2.4%.

**Table 12. Differences between modeled daily volumes and real counts of NYBPM and MATSim NYC model**

|  | East River screenline |
| --- | --- |
| NYBPM 2010 update | -2.4% |
| MATSim NYC model | 2.6% |

## 4.4 Validation

We validated the calibrated model by comparing the simulation output transit station ridership with observed turnstile count data as well as with volumes on key corridors.

### 4.4.1 Validation data

Two data sources are adopted for validation: 2016 Average Weekday Subway Ridership data (MTA, 2018) and 2014-2018 Traffic Volume Counts data (NYC DOT, 2019). The subway ridership data incorporates the average weekday ridership per subway station across the city. The ridership refers to the number of passengers entering the station, including passengers transfer from other stations. Passengers transferring in the same station are not incorporated. We selected 10 stations of the city as reference (shown in Figure 22). The validation results of transit station ridership are presented in Table 13. The difference of total daily ridership is only 8%.

**Figure 22. Subway locations for validation.**

**Table 13. Comparison of simulated and observed daily ridership of 10 stations**

| Station | Real | Simulated | Difference % |
|---|---|---|---|
| 14 St - Union Square | 106,718 | 97,825 | -8% |
| Grand Central - 42 St | 158,580 | 170,025 | 7% |
| Penn Station - 123 & ACE | 173,108 | 256,825 | 48% |
| Times Square | 202,363 | 191,425 | -5% |
| Fulton St | 85,440 | 83,025 | -3% |
| Canal St | 70,806 | 78,250 | 11% |
| 59St - Columbus Circle | 73,836 | 75,050 | 2% |
| 34 St - Herald Sq | 125,682 | 124,500 | -1% |
| Atlantic Av-Barclays Ctr (Brooklyn) | 42,711 | 59,350 | 39% |
| Jackson Hts-Roosevelt Av (Queens) | 52,296 | 41,200 | -21% |
| **Average** | **1,091,540** | **1,177,475** | **8%** |

The 2014-2018 Traffic Volume Counts data was collected by NYC DOT for validation of NYBPM. The data consists of hourly volumes of 597 locations across the city from 2014 – 2018. To validate the MATSim NYC model, the volume counts in 2016 of 15 locations are selected (listed in Table 14). As the red links show in Figure 23, some locations (e.g. 3 AVENUE) have more than one count facility. When matched with those facilities in the MATSim-NYC network, 42 links were selected. The daily volumes of the 42 links were compared and the relative difference between simulated volumes and real counts is 39.8% on average. The median difference is 29%.

**Table 14. Locations for link volume validation**

| ID | Location | ID | Location | ID | Location |
|----|----------|----|----------|----|----------|
| 1 | 10 AVENUE | 6 | CANAL STREET | 11 | MADISON AVENUE |
| 2 | 2 AVENUE | 7 | EAST 119 STREET | 12 | NORTHERN BOULEVARD |
| 3 | 3 AVENUE | 8 | FDR DRIVE | 13 | WEST 29 STREET |
| 4 | 5 AVENUE | 9 | GRAND CENTRAL PARKWAY | 14 | LONG ISLAND EXPRESSWAY |
| 5 | 9 AVENUE | 10 | GRAND STREET | 15 | BROOKLYN QUEENS EXPRESSWAY |
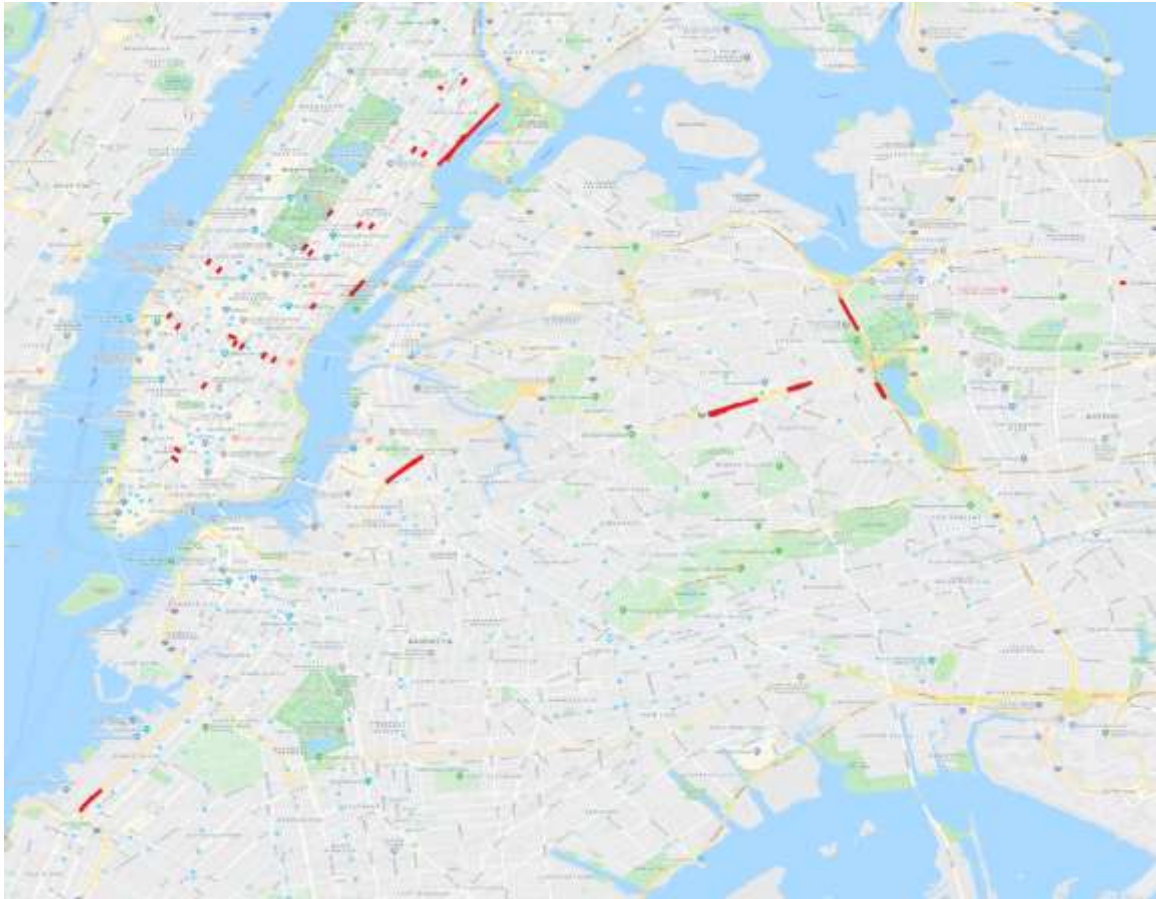
**Figure 23. Distribution of volume count facilities.**

## Section 5: Scenario analyses

We conducted five scenario analyses based on the calibrated baseline model in MATSim. Scenario One is the impact analysis of the hypothetical set-up of a new Amazon HQ in Long Island City. Scenario Two is the demand forecast of Citi Bike's expansion plan. The analyses of those two scenarios are completed based solely on the synthetic population and estimated tour-based mode choice model. Scenario Three is the evaluation of the congestion pricing policy in CBD area of Manhattan. Scenario Four is the implementation of the Brooklyn Queens Connector (BQX). Scenario Five is the deployment of autonomous vehicles in Manhattan. The last three scenarios are tested on the calibrated simulation test bed. The details of all scenarios are introduced in the rest of this section.

For our base model, we use the calibrated model with an adjustment for the fare price. Assume a passenger pays $2.75 per transit trip (unlimited plan and free transfers are assumed to be priced into that fare). The utility function of transit is adjusted and shown in Eq. (5.1) and (5.2). The disutility of fixed transit fare per trip was added into the constant of the previous utility function of transit.

$$V'_{2,k} = \beta'_{2,C} + \beta_{time,2} \times (Time_{k,2} - Time_{k,driving}) + \beta_{AT} \times AT_k + \beta_{ET} \times ET_k \qquad (5.1)$$
$$+ \beta_{WT} \times WT_k + \beta_f \times f_k$$

$$\beta'_{2,C} = \beta_{2,C} + \beta_{cost} * 2.75 \qquad (5.2)$$

### 5.1 Scenario One

Amazon planned to build a new HQ in Long Island City (LIC Development MOU, 2018). The project expected to create 25,000 new jobs in ten years and up to 40,000 new jobs in fifteen years. Although that decision has since been canceled (NBC, 2019), it presents a timely case study with well-defined parameters to study its potential effect on travel patterns as NYC continues growing its technology sector.

**Figure 24. Original planned site of Amazon's NYC Headquarters (LIC Development MOU, 2018).**

We assume the new HQ will attract employees from the "professional, scientific, and technical services" (PSTS), with North American Industry Code System (NAICS) code 54. The process flow of this scenario analysis is shown in Figure 25. First, the population is expanded with the natural growth rate 0.3% (NYC Planning, 2017) to predict the population in 2028. About 8,023 new people will join the PSTS industry for the whole city under the natural growth, of which 8.01% (643 in total) are attracted by Amazon. The reminder of 25,000 new jobs come from outside the city. Then, socio-demographic attributes and agendas are randomly assigned to those increment of population. Amazon workers receive attributes from PSTS industry while others receive attributes from other industries. Amazon workers have the simplest agenda: 8:30AM from home to work and 5:30PM from work to home. Others take the agendas as the same as the existing population excluding PSTS workers.
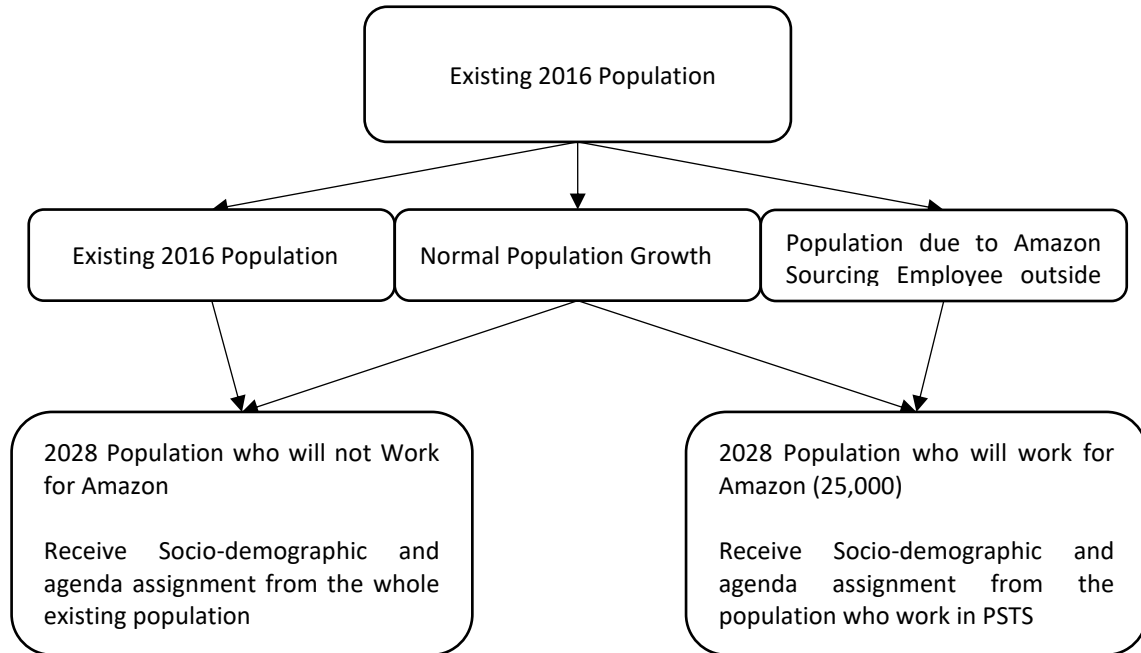
**Figure 25. Process flow of experimental design.**

By using a synthetic population, we can adjust specific individuals by employment industry. As a result, the spatial distribution of potential employees can be modeled as shown in Figure 26.
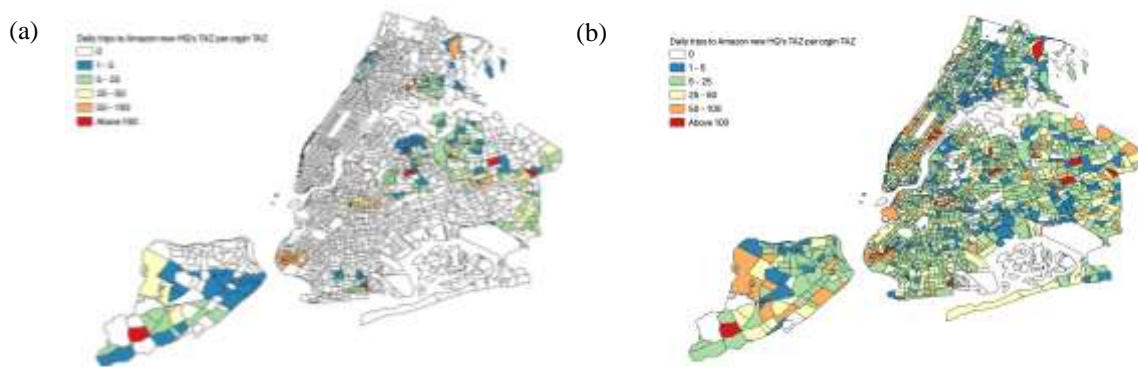


**Figure 26. Spatial distribution of home locations for workers in TAZ 362 (a) in 2016, and (b) in 2028 with Amazon HQ relocation.**

The mode choices of the increment of population are simulated based on the mode choice model. The prediction is presented in Table 15. A dramatic increase is predicted with the new HQ. The demand for taxi and FHV is expanded by more than four times, with the ridership of transit increased nearly three times. This prediction can act as a reference for policymakers to plan the improvement of infrastructure such as ensuring sufficient capacity for transit facilities nearby.

**Table 15. Mode share of Amazon workers in 2016 and 2028**

| | | Driving | Carpool | Transit | Taxi | Bike | Walk | FHV | Citi Bike | Total |
|---|---|---|---|---|---|---|---|---|---|---|
| Number of trips | 2016 | 6519 | 1262 | 10,716 | 266 | 176 | 2144 | 143 | 34 | 21,260 |
| | 2028 without Amazon | 6749 | 1316 | 11,106 | 272 | 181 | 2220 | 145 | 37 | 22,026 |
| | 2028 with Amazon | 20,081 | 3368 | 42,254 | 1393 | 848 | 3120 | 773 | 189 | 72,026 |
| Change in percentage | 2028 without Amazon | 3% | 4% | 4% | 2% | 3% | 3% | 1% | 8% | 3% |
| | 2028 with Amazon | 208% | 167% | 294% | 424% | 382% | 46% | 441% | 456% | 239% |

A further advantage of using a synthetic population is that a time-of-day analysis can be easily conducted, as shown in Figure 27. The new HQ is predicted to increase total trips from 5,000 to 8,000 in the morning peak and from 3,000 to 8,000 in the afternoon peak. Late night trips would also expand.

## Work Trips to and from TAZ 362 without Amazon



(b)

## Work Trips to and from TAZ 362 with Amazon
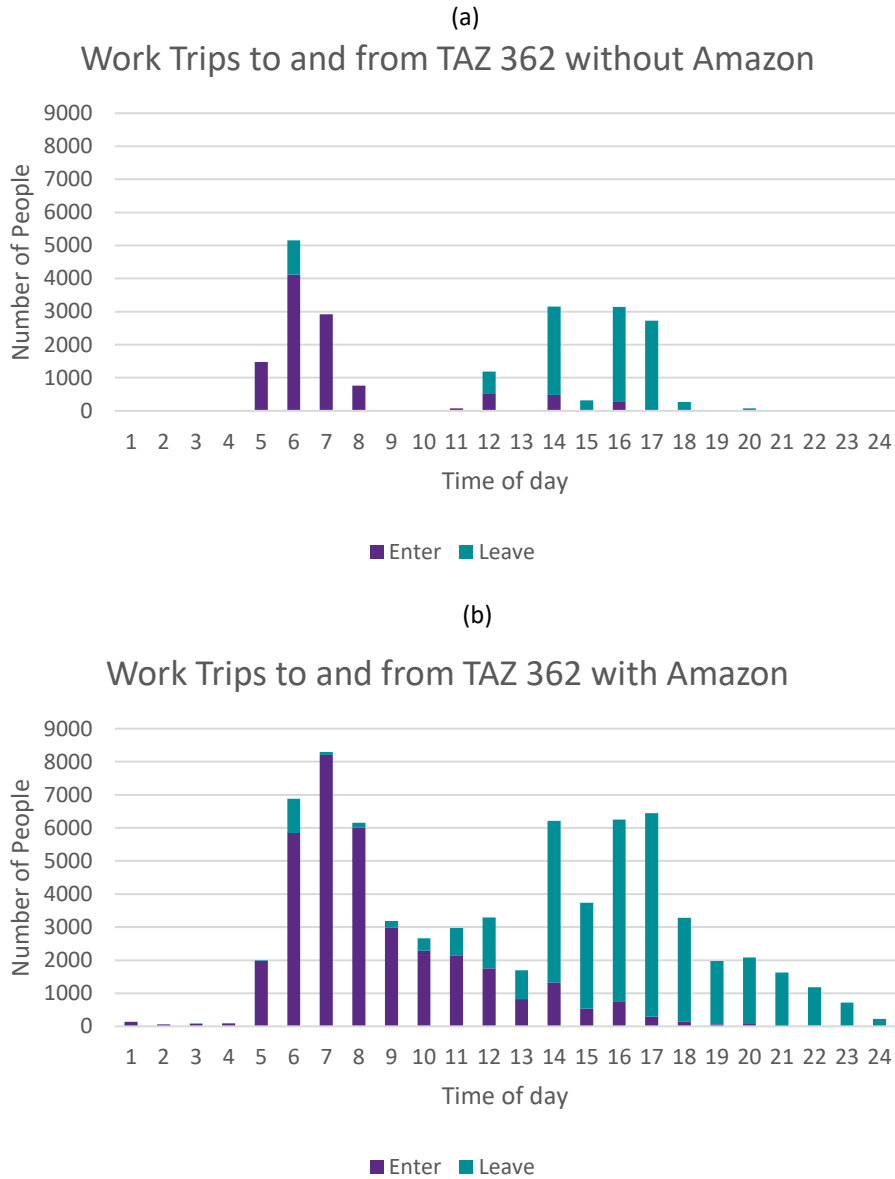


**Figure 27. Time-of-day distribution of inbound and outbound trips at TAZ 362 in 2028 (a) without Amazon and (b) with Amazon.**

## 5.2 Scenario Two

Citi Bike proposed plans in 2019 to expand its service area to double its size by 2023. The expansion plan is shown in Figure 28. We estimated the demand attracted by the expanded service assuming that the level of service of the system remains the same. The parameters

estimated for the bikeshare mode should still be applicable in the expanded system condition, with users from more zones having access to the mode.
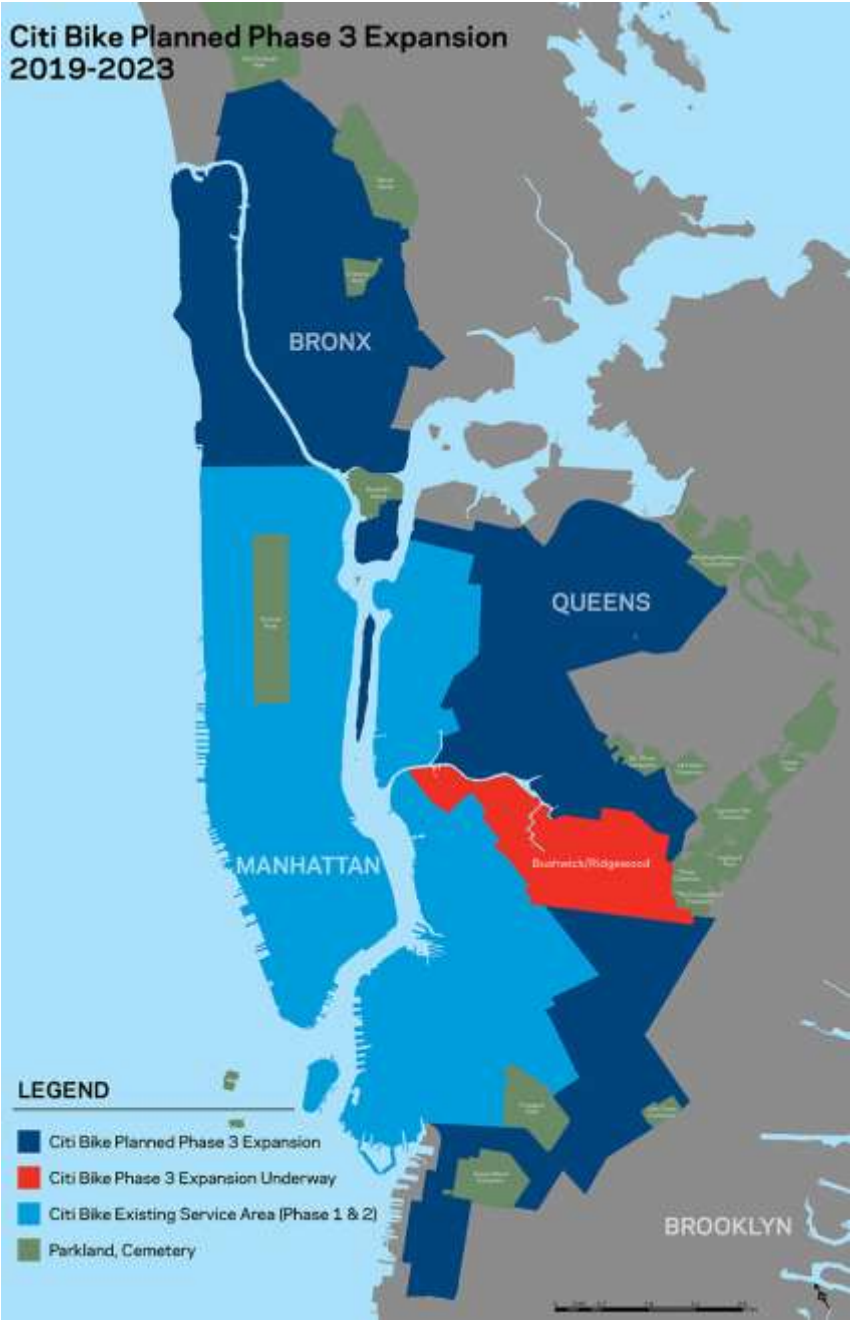


**Figure 28. Planned Citi Bike service area expansion (source: Citi Bike, 2019).**

We re-simulated the mode choices of the synthetic population with different Citi Bike service areas and presented the mode share in Table 16. With service area doubled, the demand for Citi bike also doubled, increasing from 0.15% (47,475 daily trips) to 0.30% (91,052 daily trips). When expanding the service area to the whole city, the increment of demand only increased to 0.48% (147,308 daily trips), which is about three times the original service demand.

**Table 16. Mode share from synthetic population under different expansion scenarios**

| Mode | Driving | Carpool | Transit | Taxi | Bike | Walk | Citi Bike | FHV |
|------|---------|---------|---------|------|------|------|-----------|-----|
| Original | 22.69% | 5.39% | 36.23% | 2.12% | 1.86% | 30.63% | 0.15% | 0.92% |
| 2A: Citi Bike's expansion plan | 22.68% | 5.39% | 36.16% | 2.12% | 1.85% | 30.58% | 0.30% | 0.92% |
| 2B: Whole city | 22.67% | 5.37% | 36.09% | 2.11% | 1.85% | 30.51% | 0.48% | 0.92% |

A spatial analysis can be conducted since we model each individual that chooses Citi Bike for a trip. This is shown in Figure 29.
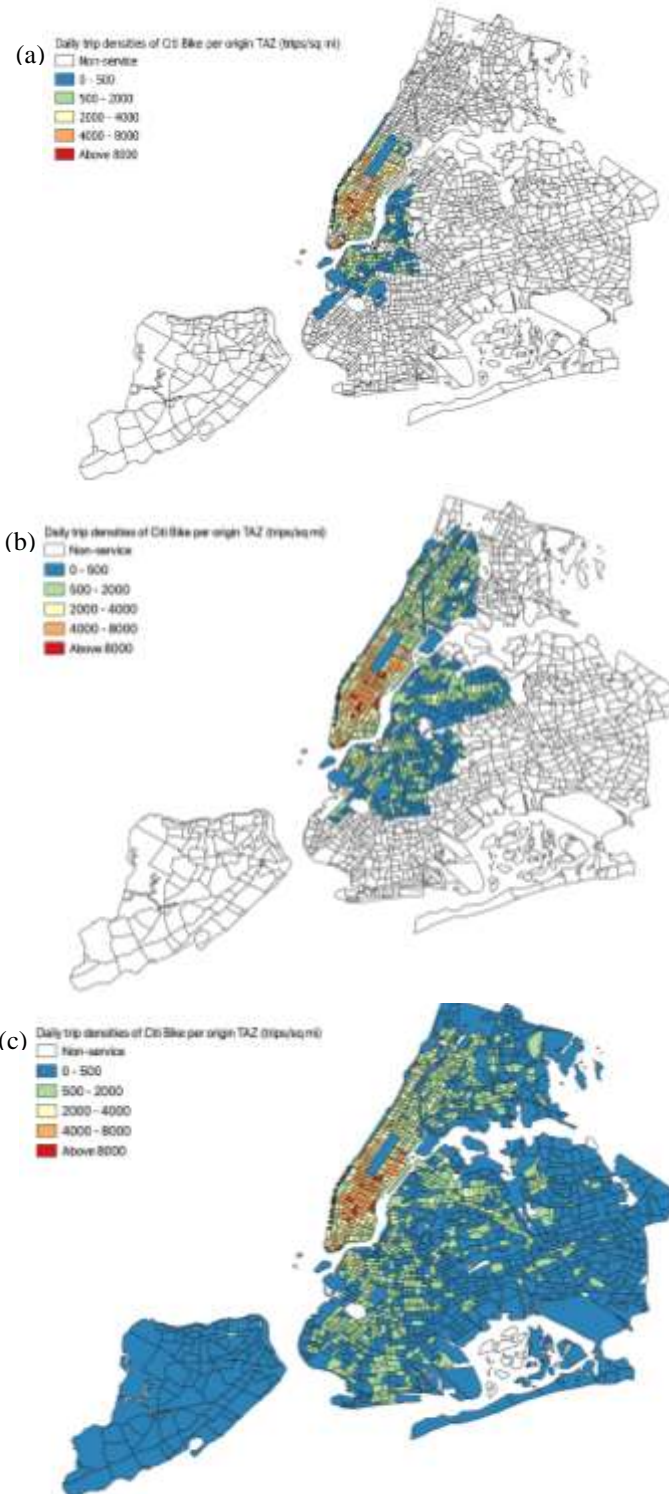
**Figure 29. Distribution of synthetic daily Citi Bike trip densities per origin zone under (a) original service area, (b) Citi Bike's expansion plan, and (c) the whole city as the service area.**

## 5.3 Scenario Three

In the following sections, the scenarios all use the calibrated MATSim-NYC model as the base scenario. When running alternative scenarios to compare against a base scenario, the set of plans at the end of the base scenario runs for the population is used to initiate the new scenario run to represent their acquired knowledge of their options.

NYC plans to implement a congestion pricing policy to charge vehicles entering Manhattan under 60th Street to relieve congestion and raise money to support public transit (Holland and Shah, 2019). The charge area is bounded with red lines in Figure 30.



**Figure 30. Charging area in Manhattan.**

We study the scenario using MATSim-NYC. The advantage of using MATSim-NYC to evaluate these scenarios is that the travelers can experience queue delays in a single day's simulation due

to changes in spillback effects from the congestion pricing that cannot be captured using a static assignment model. Furthermore, the day-to-day adjustment in MATSim-NYC allows travelers to adjust their schedules and departure times, which is more realistic than a static model which forces travelers to, at best, substitute trips with other modes or routes. Third, as the model is multi-agent and linked up with the experienced travel agendas on the dynamic traffic network, we can compute the output utility change to each traveler to compute the social welfare effect of a policy. This has powerful economic value to evaluating emerging transportation technologies and policies.

The Regional Plan Association (RPA) published a report about the impacts of congestion pricing in Manhattan. Four different charging schemas were compared. We implemented the highest charging schema from that plan in our virtual test bed. Another schema tested is $14 per passenger vehicle according a new pilot program (Holland and Shah, 2019). The simulated charging schemas are presented in Table 17. All prices are charged two-way, which is consistent with RPA's report.

**Table 17. Simulated charging schemas of congestion pricing**

| Schema | 1 | 2 |
|---|---|---|
| Peak (6-10AM, 2-8PM) | $9.18 | $14 |
| Off-peak (5-6AM, 10AM-2PM,8-11PM) | $3.06 | $3.06 |
| Night (11PM-5AM) | $3.06 | $3.06 |

The congestion pricing was implemented using MATSim's extension "Road Pricing". The simulations were run on a desktop with Intel(R) Xeon(R) CPU E5-2637 v4 @ 3.50GHz processors and 128GB RAM. Each implementation of schema ran with 100 iterations in MATSim. The computation time is approximately 15 hours per scenario.

Considering the charging area is not the whole Manhattan, we use a different population segment definition to evaluate the impact of the policies. Two segments are defined as "Charging-related" vs. "Non-charging-related". A person who has at least one trip related to the charging area belongs to the Charging-related segment (including travelers making trips

completely within the charging area without paying a cordon fee); otherwise, they belong to the Non-charging-related segment.

The trips shift for people from charging-related segment as shown in Figure 31. A significant drop in car trips is found under both schemas, where the higher price leads to a larger drop. Compared to the 59,000 decrease of daily car trips from RPA, our simulation indicates a 127,000 decline under the same schema (Schema 1). Trips of all modes except for transit and walk decreased after charging the congestion price. These outcomes are in line with expectations since Manhattan would become less congested and more people will use transit instead of car.

The daily and annual revenues collected under each schema are calculated and presented in Table 18. The daily revenues are obtained from the simulation and the annual revenues are calculated by aggregating the daily revenues of weekdays through a year (261 days), with 4% legislated exemptions, $113M operating cost, and $30M deduction from a technical memorandum (RPA, 2019). The results are consistent with RPA's projection, although our simulation reports double the reduction in cars shifted to other modes.
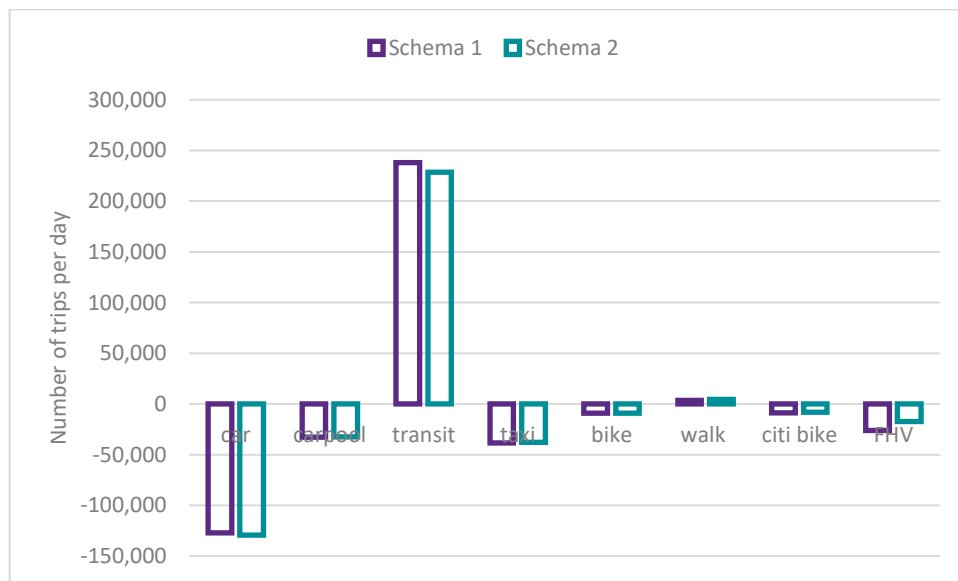


**Figure 31. Daily trip shifts after charging congestion price for charging-related segment**

**Table 18. Revenues collected under each schema**

|  | Schema 1 | Schema 2 | RPA's proposal |
|---|---|---|---|
| **Daily revenue** | 4.91M | 6.75M | N/A |
| **Annual** | 1.09B | 1.55B | 1.09B |

The changes in consumer surplus for travelers relative to the baseline scenario are estimated and presented in Table 19. When calculating the changes in people's daily utilities, the utility of performing activities is excluded, i.e. the utility calculated by Eq. (4.2a) is subtracted from the daily utility. This is because that portion of the utility is not calibrated unless panel travel surveys are conducted over multiple weeks to observe changes in activity participation per individual (Chow and Nurumbetova, 2015). Here we only focus on the impact of congestion pricing on the travel disutility. First, people from both population segments (charging-related and non-charging-related) have an increase in consumer surplus, which indicates a positive impact on people in NYC from congestion pricing. People from the charging-related segment benefit more than those from the non-charging-related segment, by an increase of 53 – 55%. This implies that the congestion pricing provides a net savings in travel times for all the travelers within the charging area that significantly overcompensates for the cost of the charge on people crossing it. The results endorse the decision of charging congestion price in Manhattan. Furthermore, the revenues collected from charging a congestion price can be used to improve social welfare, e.g. invest in the public transit system to improve the level of service, and suggest that redistribution of toll revenues should focus on outer boroughs transit service. Second, we see that Schema 2 results in a lower net benefit than Schema 1. This implies that the $14 charge may be too high compared to the $9.18 charge, although it would further (incrementally) benefit folks in the charging area. This result suggests the importance of using policy tools like MATSim-NYC to help design the congestion pricing policy as it can offset benefits from one population segment against another. This finding would not have been possible using a static network policy tool.

**Table 19. Average change in daily consumer surplus ($) per traveler by segment**

|  | Charging-related | Non-charging-related | Citywide |
|---|---|---|---|
| Schema 1 | +21.99 | +14.37 | +16.52 |
| Schema 2 | +22.01 | +14.21 | +16.41 |

Another finding from our analysis that is possible due to the use of an agent-based simulation is tracking the mode shifts of the car drivers under congestion pricing. The results are presented in Figure 32. About 72% of car trips are maintained, 15% shifted to transit, 10% switched to FHV and taxi.
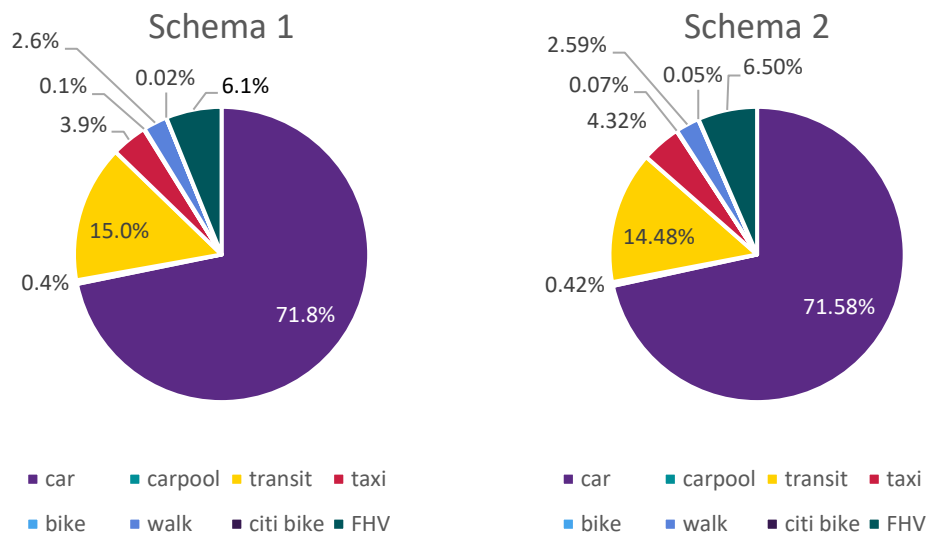


**Figure 32. Mode shift of car drivers after charged congestion price under (a) Schema 1 (b) Schema 2.**

Based on the versatile output of MATSim, the simulated hourly volumes of each link are available. The spatial distributions of average hourly volume in AM peak hour (6AM – 10AM) before and after congestion pricing are shown in Figure 33. After charging congestion pricing, the volumes in midtown and downtown Manhattan have a slight decline, while the volumes in the area above 60th Street, which is outside the charging area, increase. The results are aggregated to daily average; specific times of day can be output.

**Figure 33. Average hourly volume distribution (a) before congestion pricing and (b) under Schema 2.**

## 5.4 Scenario Four

BQX is a proposed streetcar service connecting Astoria in Queens and Red Hook in Brooklyn, as shown in Figure 34. The city's Economic Development Corporation and NYC DOT have a plan

to release the final design by 2023 and finish construction in 2029 (Robbins, 2020). The BQX is anticipated to have an initial daily ridership of 50,000 and up to 90,000 after a few decades. According to the design report of BQX (BQX, 2018), the service time will be 5AM to 11PM, with five minutes headway in peak hours (6:30AM – 9:30AM; 4:30PM – 7:30PM) and ten minutes headway in off-peak hours. Assuming the travel speed of BQX is 8mph, we simulated the BQX with our test bed on a desktop with Intel(R) Xeon(R) CPU E5-2637 v4 @ 3.50GHz processors and 128GB RAM. The computation times are around 13 hours.



**Figure 34. Plan of the Brooklyn Queens Connector (source: BQX, 2019).**

The simulated daily ridership of BQX is 112,775, which is more than twice of the proposed daily ridership (50,000). The results of the simulation indicates that the BQX might be more attractive than expected. The simulated volume and proposed volume across all stations are

presented in Figure 35. The distribution of simulated volume is similar to the proposed volume although the magnitudes are much greater.
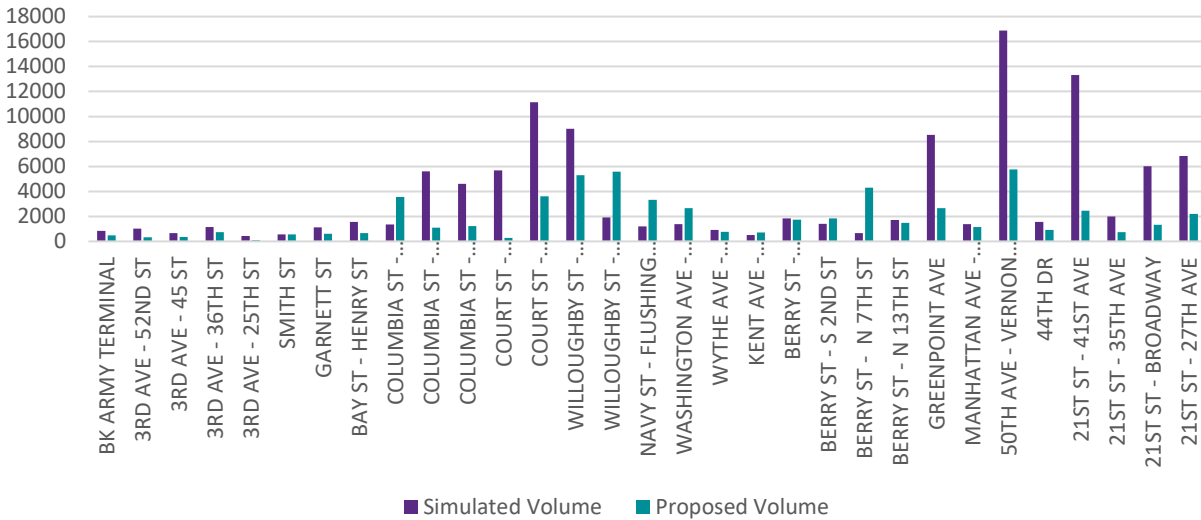


**Figure 35. Simulated volume and expected volume across all stations of BQX.**

The north-bound vehicle load profile in the morning peak hour is presented in Figure 36. The results show that the route's peak load occurs around the 50th Ave – Vernon Blvd station.
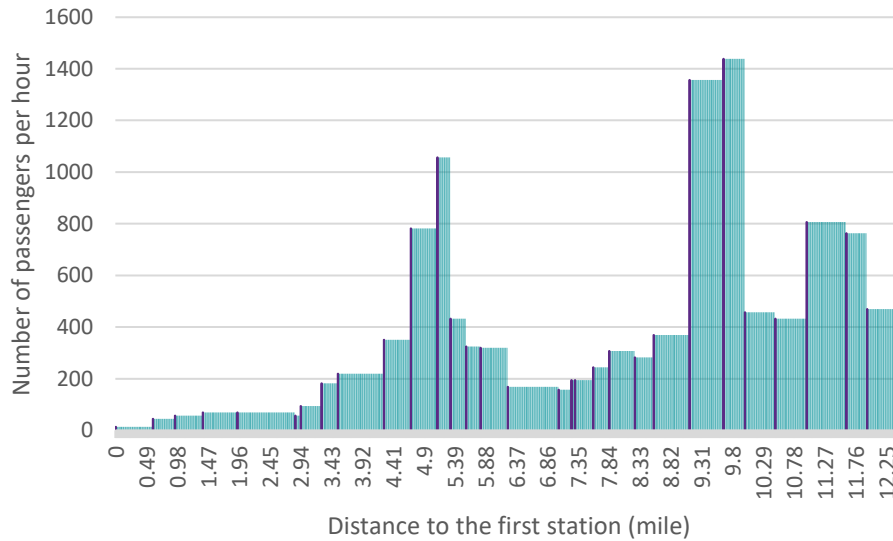
**Figure 36. Simulated north-bound load profile in AM peak.**

By tracking the agents, we see the mode shift of BQX riders in Figure 37. Most of the BQX riders switched from other transit routes. About 16% of passengers were drivers who gave up driving private car and shifted to BQX. This suggests that it's primarily attracting transit users who find that BQX improves their journey's level of service. The around 16% shift means that BQX would take 18,000 drivers off the road to take transit per day.
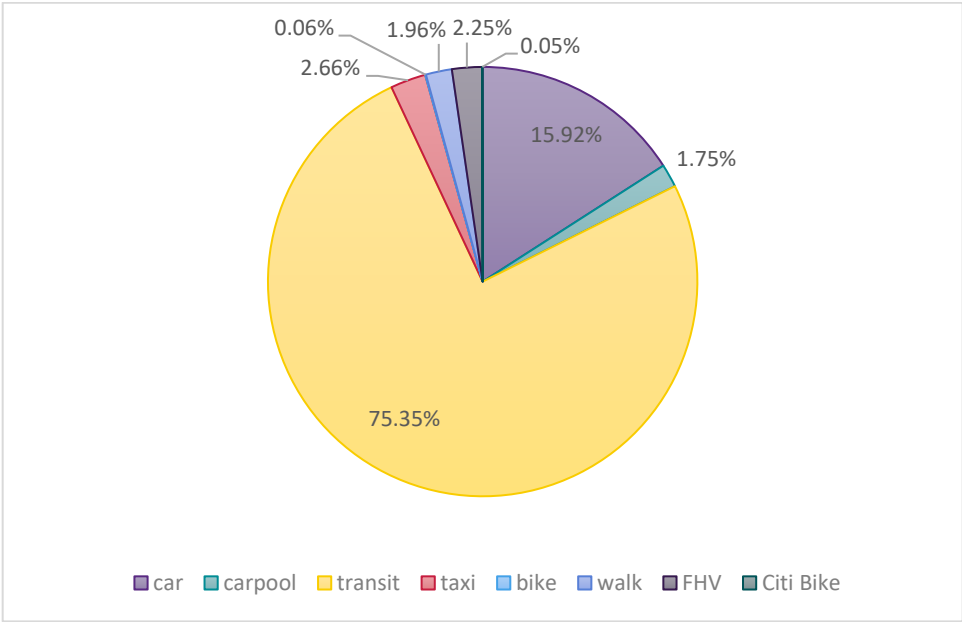
**Figure 37. Mode shift of BQX riders.**

## Section 6: Further extension

### 6.1. MATSim traffic flow model improvement

Traffic flow model and its parameters have critical impacts on the simulation performance, in this study, we introduce a method to improve the default traffic flow model and calibrate its parameters in MATSim.

MATSim uses queuing models to capture the queue formation, spillback and dissipation (e.g. point queue, spatial queue). Although the point queue and spatial queue model are mainly used in MATSim, however, the intra-link interaction is ignored because when a vehicle leaves the upstream end of a link, the space immediately becomes available, even if this is not a very realistic assumption from the traffic flow theory perspective. To address this problem, we modify the default traffic flow model in MATSim to incorporate more realistic link dynamics. Agarwal et al. (2018) integrated the link transmission model (LTM) model into the existing MATSim spatial queue model by introducing a concept called "backward traveling hole", also known as the double-queue model. We extend the traffic flow model in Agarwal et al. (2018) by relaxing the assumption of a fix backward hole traveling speed by making the hole speed heterogeneous among links based on real traffic data.

In addition, due to the limitation of available traffic flow data in New York City, we propose a clustering-based calibration framework to calibrate the parameters of traffic flow model. We first employ a clustering algorithm to extract typical traffic patterns from link-based traffic speed profile. Using these clusters, traffic flow parameters of individual links belonging to a specific cluster can be calibrated using speed-flow data available for a subset of all the links in NY network.

#### 6.1.1. Data

Historical traffic speed data is shared by INRIX with the approval of NYCDOT. INRIX is a private company that provides data for transportation research and city planning (http://inrix.com/). The speed data is aggregated to a 5 min time interval. Furthermore, to calibrate the parameter of a given traffic flow model, the relationships among traffic flow $q$, speed $v$ and density $k$ are needed. The speed-volume data from 281 links that are part of the NYC Midtown in Motion (MiM) project, which became operational in 2011, are used. The available sensor data is from a 110-square block area or "zone" from 2nd to 6th Avenues and

from 42nd to 57th streets. The link speed-flow data from the 281 segments were collected through Nov 1st to Nov 7th of 2011 in intervals of 1 minute.

## 6.1.2. Modify the traffic flow model

In Agarwal et al. (2018), the space freed from a leaving vehicle is called a "hole" and travels opposite to the direction of the traffic flow. In unsaturated conditions, flow increases linearly with density, while in saturated conditions, flow decreases linearly with density. A maximal value of flow is equal to:

$$\hat{q} = \frac{v_f v_{hole} \rho_{jam}}{v_f + v_{hole}} \tag{6.1}$$

where $\hat{q}$ is the maximum flow, $v_f$ and $v_{hole}$ are free flow speed and backward speed respectively, $\rho$ is density, $\rho_c$ is critical density and $\rho_{jam}$ is jam density. The hole's travel time ($t_{hole}$) is calculated as: $t_{hole} = l_{eff}/v_{hole}$, where $v_{hole}$ is the travel speed of the hole, and $l_{eff}$ is the effective length of the vehicle.

A constant hole speed of 15 km/h is assumed in Agarwal et al. (2018). We modify the model to relax this assumption and make the hole travel speed heterogeneous among links. The maximum density in MATSim equals one over the length of a vehicle (effective cell size attribute of the links element) for a single-lane link and needs to be multiplied with the number of lanes (permlanes attribute of the link element). Then under free speed condition ($\rho \leq \rho_c$), the flow ($q$) is $q = v_f \rho$. If the link is congested ($\rho_c \leq \rho \leq \rho_{jam}$), the flow ($q$) is $q = v_{hole} (\rho_{jam} - \rho)$. At critical density $\rho_c$, the flow from the free-speed branch and congested branch will be equal:

$$v_f \rho_c = v_{hole} (\rho_{jam} - \rho_c) \tag{6.2}$$

Thus, the backward hole traveling speed is estimated as:

$$v_{hole} = \rho_c * v_f /(\rho_{jam} - \rho_c) \tag{6.3}$$

### 6.1.3. Clustering-based algorithm for parameter calibration

We employ the hierarchical clustering algorithm to group links based on their speed profiles. The basic agglomerative hierarchical clustering algorithm is as follows: a) consider each of the $n$ objects as a unique cluster; b) merge clusters based on their similarity measurement, Euclidean distance; 3) repeat step b repeatedly until a desired number of clusters is achieved.

The three variables needed to be calibrated in the modified traffic flow model are free flow speed, flow capacity and critical density. Free-flow speed is "practically determined as the average speed of passenger cars in conditions of low traffic flow rates" (Erdelić et al., 2015). Since there are no explicit free-flow speed data available, we estimate the free-flow speeds using nighttime speeds from INRIX when traffic moves freely without congestion, where nighttime is defined as the time interval between 01:00h and 05:00h. The flow capacity is estimated by assigning the maximum value of flow crossing a given link. Then the flow capacity value is horizontally projected to the free-flow line in the triangular fundamental diagram. The intersection is the critical density, with the free-speed branch on the left side and congested branch on the right side. The hole travel speed is then obtained from Equation (6.3).

### 6.1.4. Model performance discussion

To test the performance of the modified model, we use 0.1% and 1% samples of the 8.2 million synthetic population. In the configuration file of the simulation, we set the parameters of activities as default and the parameters of travel modes the same as the mode choice model in the synthetic population. The traffic speed data generated 9 representative clusters. The relative accuracy for each link is the difference of average link speed between simulated and observed data (INRIX speed data). Then the difference is averaged through all the links to obtain the average relative accuracy.

The default model refers to the basic queue model in MATSim while the improved model refers to the modified model. We ran 20 iterations of the simulation for each scenario: a) 0.1% population with default model; b) 0.1% population with modified model c) 1% population with default model; d) 1% population with modified model. The result of this comparison is shown in Table 20.

Clearly, the results show that the improved traffic flow model with calibrated link parameters can significantly increase the simulation accuracy while having little impact on the overall computational time.

**Table 20. Performance of traffic flow model calibration**

| | Computation time (hh:mm:ss) | | relative error of link average speed | | Improvement |
|---|---|---|---|---|---|
| | Default model | Modified model | Default model | Modified model | |
| 0.1% population | 0:10:38 | 0:10:48 | 52.15% | 26.47% | 23.68% |
| 1% population | 1:10:17 | 1:16:43 | 47.86% | 29.49% | 18.37% |

## 6.2. Autonomous vehicle fleet

Testing of Autonomous Vehicle (AV) in an urban setting can be cost prohibitive and sometimes fatal (Aupperlee, 2017). MATSim-NYC provides a cost-effective way to test AV routing and operating strategies in an urban environment. MATSim has shown promising results when simulating large-scale scenarios for transport planning with agent-based micro simulations in a reasonable time. It is able to handle not only the traffic patterns but also detailed descriptions at the single agent level (Balmer et al., 2009).

MATSim can also be used to test the feasibility of AV fleet deployment (Hörl et al., 2019). The success of an AV operator can depend on the selection of its service area. Deploying few vehicles in areas of high demand might drastically increase the wait times of users and limit AV usage. A small fleet size will have smaller capital expenditures but inevitably increases wait times. An efficient use of vehicles restricts the number of empty VMT, but also increases wait times, as vehicles without a passenger on board cannot be relocated to high demand locations. As AV fleets are becoming a reality, there is need to address their operational efficiency in an urban environment through agent-based simulation like MATSim-NYC.

The simulation of AV fleets or Autonomous Mobility-on-Demand (AMoD) (Hörl et al., 2019) in MATSim uses the Dynamic Vehicle Routing Package DVRP (Maciejewski et al., 2017). MATSim can simulate riders' daily plan to assign a score according to the durations and distances covered in the mode, their arrival times, waiting times, their stay durations at an activity and other dimensions. We investigate the package in MATSim-NYC.

## 6.2.1. Methodology

A typical simulation run using the AMoD extension in MATSim includes the steps depicted in Figure 38.
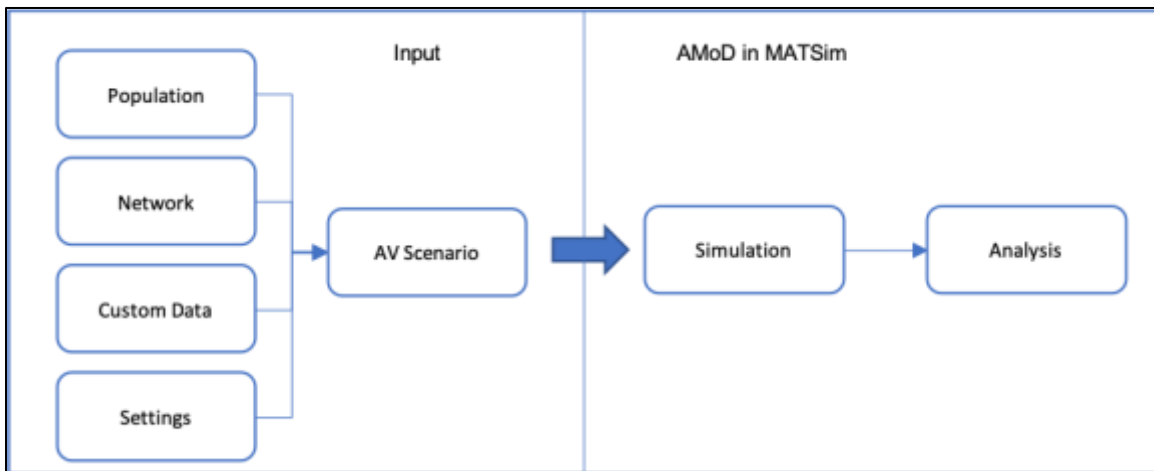


**Figure 38. Overview of the AMoD simulation process.**

The input to an autonomous mobility-on-demand simulation scenario consists of a network containing road information in the MATSim-native XML format. It includes all nodes and links including their spatial position and parameters such as the free-flow speed and link capacity. Furthermore, the scenario consists of a population of agents, each agent having travel and activity plans on the network. Custom data such as manually set link speed reductions, a public transportation network, cost models or other can be added to the scenario. Finally, a wide range of settings can be used to modify the scenario. These settings include for instance the choice of the AMoD dispatching logic or pricing structure. The AMoD dispatching logic defines how to handle requests by agents, who choose to use an AV service. Th pricing structure can either be implemented individually or can be based on a standard implementation, where one can define monetary costs per time and distance, as well as the billing intervals.

A complete scenario is then processed using the AMoD extension in MATSim using the dispatching logic and pricing structure formulated in the input part. In addition to the MATSim output results, the AMoD extension creates a custom scenario viewer as displayed in Figure 39.
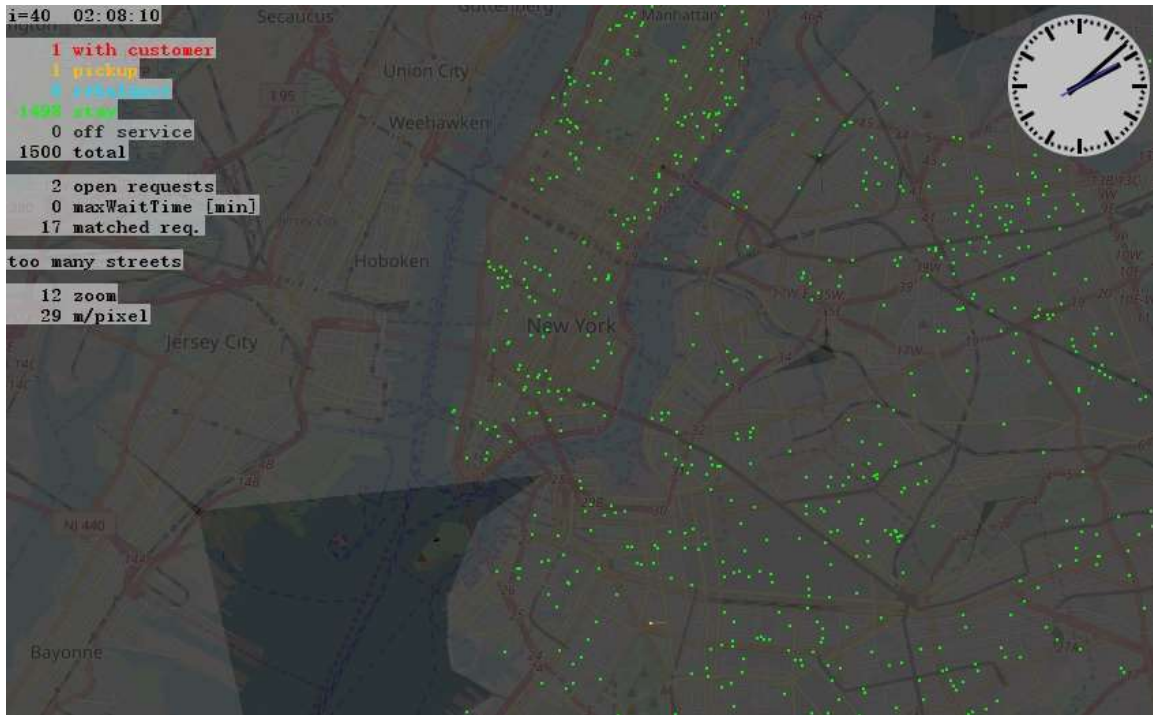
**Figure 39. AMoD scenario visualization.**

## 6.2.2. Simulation results

The simulation was run with a 0.1% sample population of NYC (about 8000 agents) and an autonomous fleet of 100 fleet vehicles to test its proof-of-concept for use in MATSim-NYC. The simulation results are presented in Figure 40 – 43.
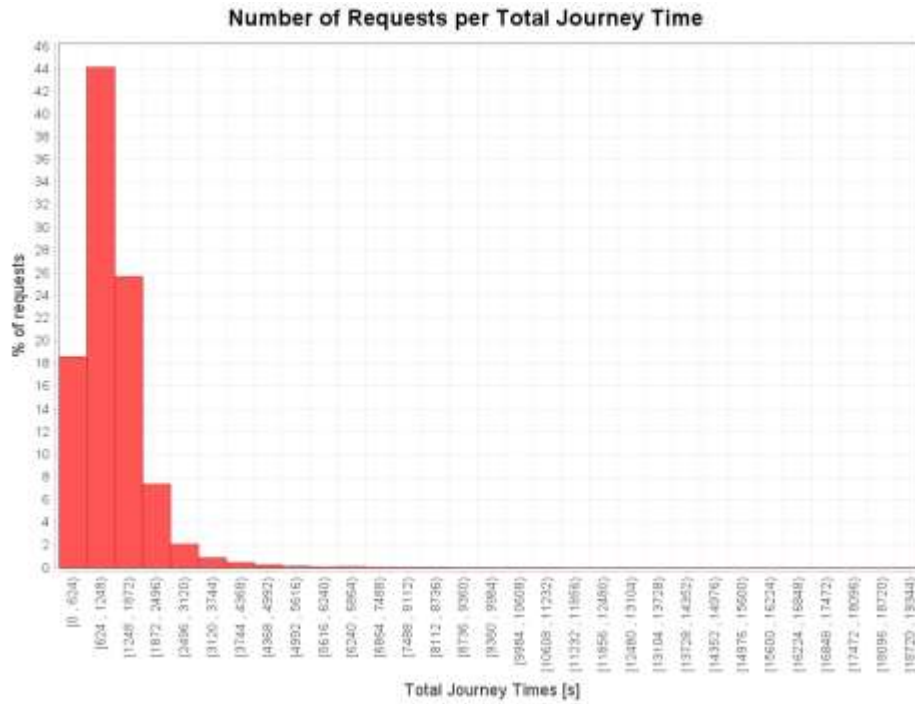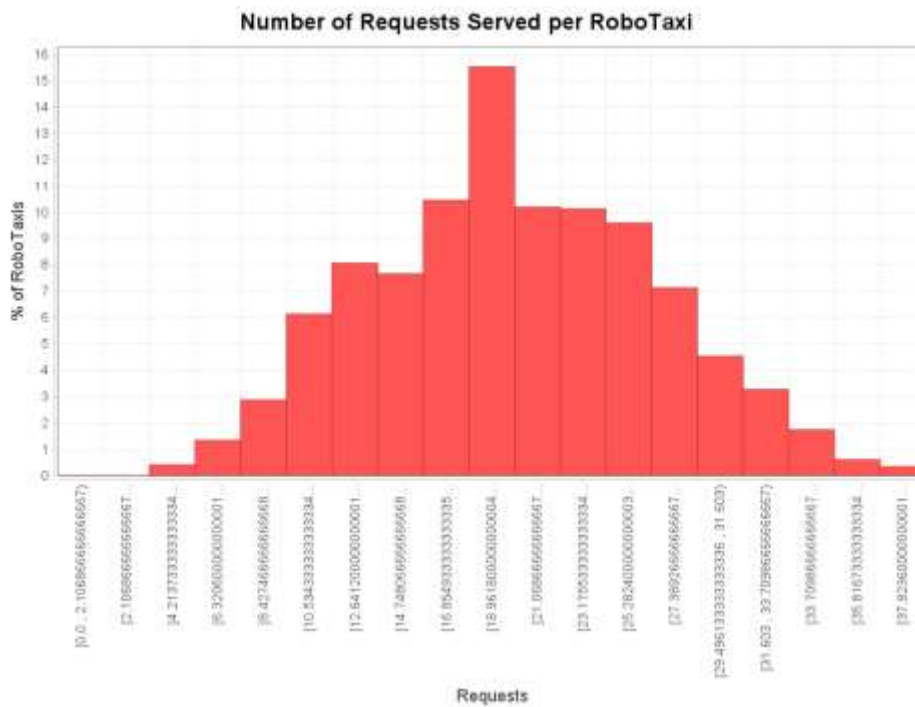
**Figure 40. Distribution of request per total travel time.**



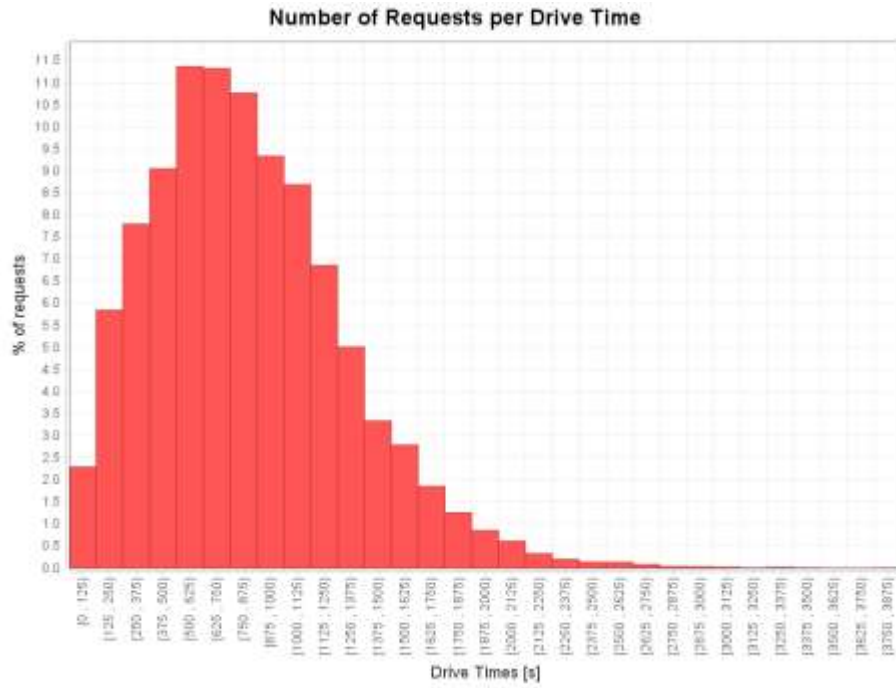**Figure 41. Distribution of requests served by autonomous taxi.**

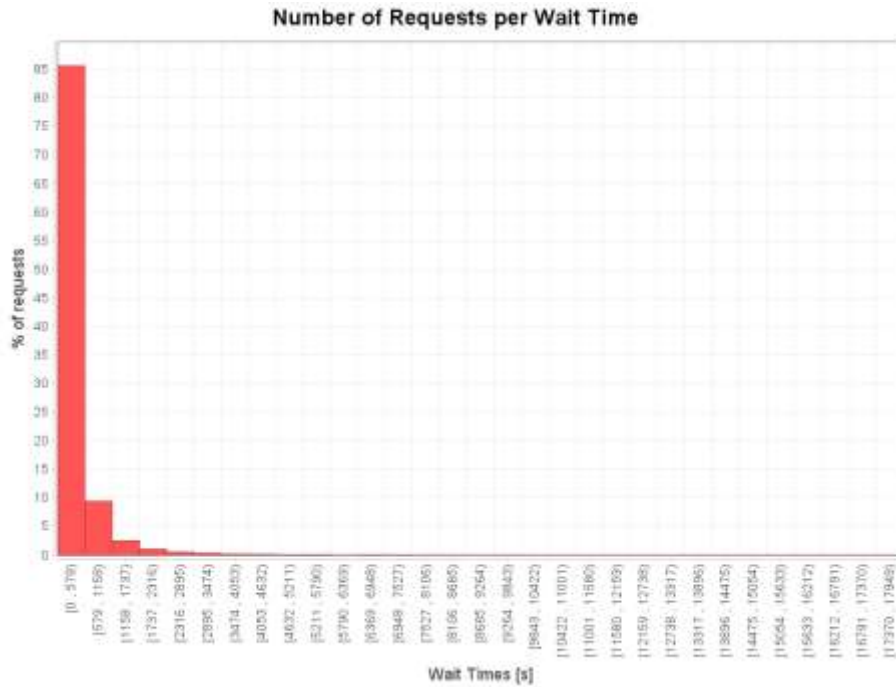**Figure 42. Distribution of request per drive time.**



**Figure 43. Distribution of requests per wait time.**

## 6.3. Multimodal router for MATSim

MATSim does not generate multimodal routes in its default package. However, multimodal travel, particularly in the context of Mobility-as-a-Service (MaaS), is rather important in cities like NYC (Djavadian and Chow, 2017b; Ma et al., 2019; Pantelidis et al., 2019). Trips combinations of one or more modes with walking, biking, transportation and driving. There are a few specialized open-source routing tools. We investigated R5, OpenTripPlanner (OTP), and the SBB-extension of MATSim. Using passenger information and transportation network provided, these routing engines are planning trips with the combination of different mode and time windows by multicriteria optimization.

With the growing popularity of micro mobility services such as CitiBike and Escooter, we especially focused on applying intermodal access/egress routing, which is required for door to door routing. SBB-extension can capture not only the usage of transportation system and personal car, but also the behavior of each agent for access/egress to transit. We tried to add different modes for access/egress trips to the transit stations.

### 6.3.1. R5 multi-modal router

R5, "Rapid Realistic Routing on Real-world and Reimagined networks", is a multi-modal routing engine developed by Conveyal[1]. It is an open-source project based on Java. The routing method of R5 is discussed in detail by Conway et al. (2017, 2018). On the basis of the Round-Based Public Transit Routing (RAPTOR) algorithm, R5 adopted range RAPTOR with Multi-criteria pareto-optimal search to calculate the multi-modal routes.

The R5 requires OpenStreetMap data as the road network and GTFS data as the transit network. The output is the multi-modal routes for a given OD pair.

### 6.3.2. Open Trip Planner

OTP is another open-source and cross-platform multimodal route planner written in Java. It computes the multimodal shortest path with several criteria: earliest arrival, fewest transfers, wheelchair accessibility, safety, elevation and so on. Compared with other routers, it is able to

---

[1] See details in https://github.com/conveyal/r5.

carry out analysis with amended transport data, such as amended GTFS data and modified network. It also included bike modes in multimodal routes, which is rare in route planners.

The routing algorithm of OTP is A*, which is a derived from Dijkstra's algorithm, with improvements in searching time. Raptor is also incorporated into OTP in 2018, which is able to search with multiple criteria, minimizing both arrival time and number of transfers. OTP has been implemented in multiple transportation agencies, including for New York State (see 511 Rideshare, 2020).

Figure 44 is the user interface of OTP implemented on the NYC road network. Users can either click on the map or enter coordinates to define the origin and destination.
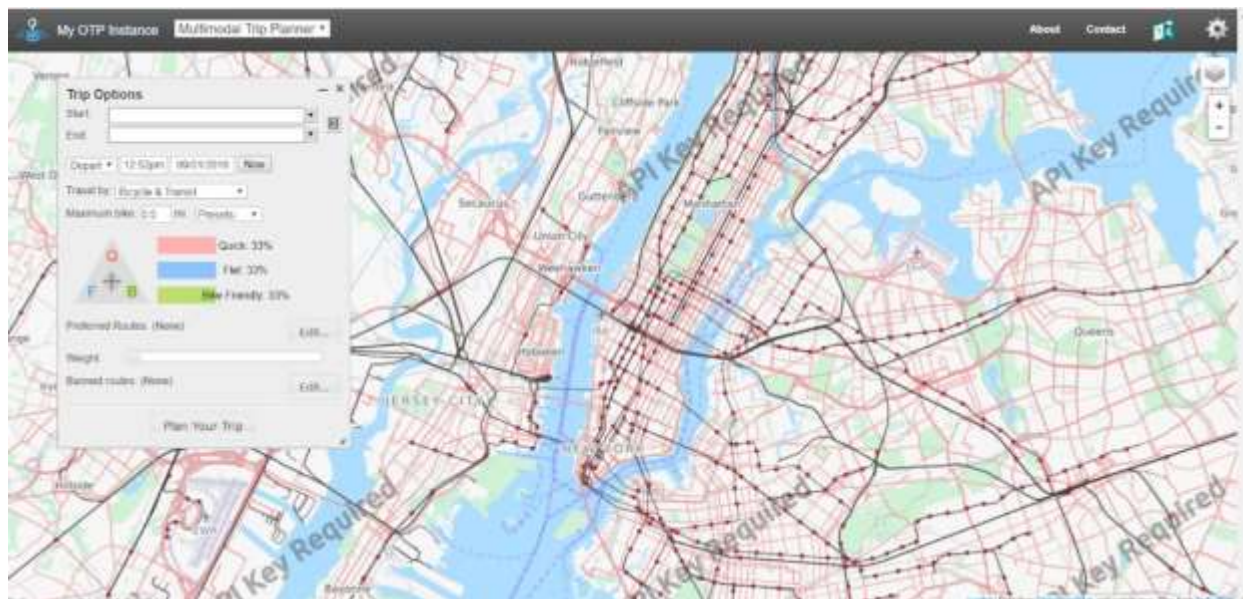


**Figure 44. User interface of Open Trip Planner.**

In OTP, the route searching is restricted by user's preferences. Users can define their preferred routes and banned routes, as well as their preferred departure/arrival time and modes. All the modes that can be selected from include:

- Transit
- Bus only
- Rail only

- Airplane only
- Walk only
- Drive only
- Park and Ride
- Kiss and Ride
- Bicycle only
- Bike and Ride
- Rented Bicycle
- Transit and Rented Bicycle

When a user selects the mode of "Transit", he or she can define a preferred longest walking distance. When a user selects a mode with bike, it will ask the user to "drag" his or her preference between quickness, flatness and bike friendliness. With the above information, 3 itineraries are generated, which are the top 3 routes searched by the criteria defined by the user as shown in Figure 45. Except for using the interface, researchers can use R to generate routes automatically with the package "otpr".



**Figure 45. A Sample Query of Open Trip Planner.**

The data that OTP needs as input includes transit data in GTFS format, street Infrastructure data from OpenStreetMap and elevation data from the National Elevation Dataset. If the modes associate with bikes are required, data on the distribution of bicycle facilities is also needed.
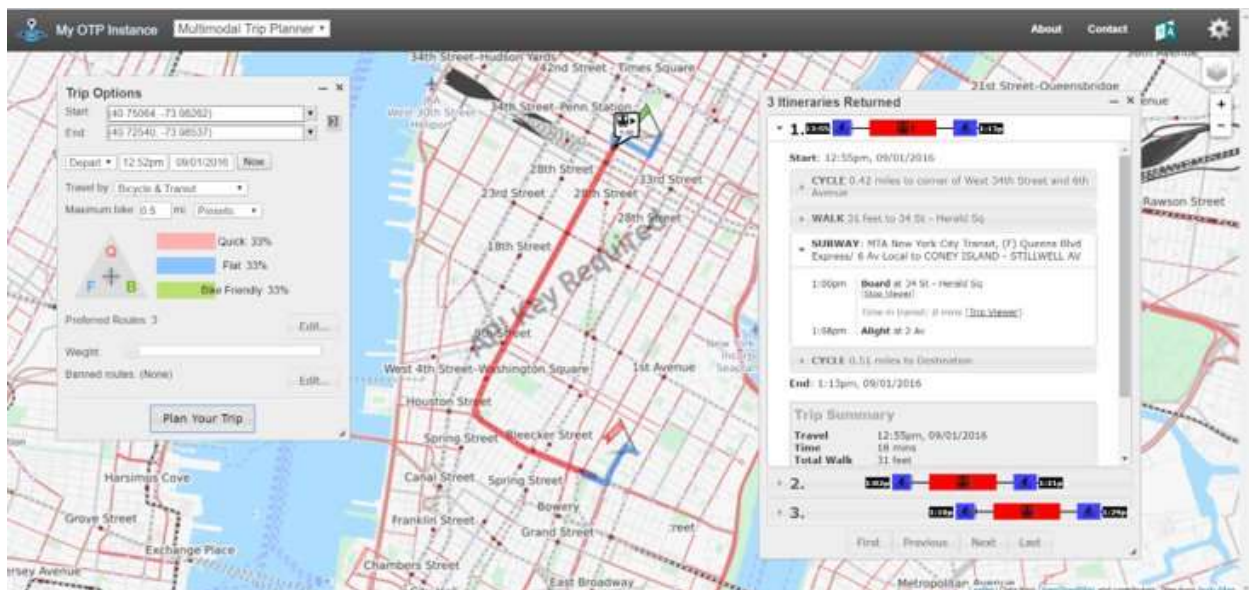
### 6.3.3. SBB-extension

The MATSim SBB-extension is provided by Swiss Federal Railways (SBB, Schweizerische Bundesbahnen). It is also based on the RAPTOR algorithm and applies several optimizations. It acts as a replacement for the default transit router in MATSim, and also provides additional features. One of those additional features, intermodal access and egress, can be utilized to generate multi-modal trips. Be defining available modes for access and egress of a transit trip and related attributes (e.g. searching radius), the extension can calculate the multi-modal routes with transit as the major mode.

### 6.3.4. Discussion

After investigating all three multi-modal routers, here are our findings. First, R5 is still problematic to be implemented in the context of NYC. More efforts are needed to look into the coding side. OTP can generate multi-modal routes for given OD pairs in NYC under several criteria. However, since the OTP is an independent router from MATSim, further efforts are needed to incorporate it into the simulation of MATSim. Third, as an extension of MATSim, it is convenient to incorporate SBB-extension into MATSim simulation, which is better than the other two routers. However, the multi-modal routes from the SBB-extension are not real "multi-modal" routes. They are transit routes with multi-modal access and egress. There are still errors when implemented with the real road and transit networks in NYC.

For next steps, our suggestion is to continue with the SBB-extension. Considering the compatibility of code, it might take much more effort to incorporate R5 and OTP with MATSim-NYC, whereas there is no such concern for the SBB-extension as a MATSim extension. It would be more efficient to customize the SBB-extension to overcome the limitations mentioned before.

## 6.4. Bike-sharing extension

The simulation of bicycles and bike-sharing in MATSim is not incorporated in the default packages. The bike trips are simulated as teleportation in our baseline model. In other words, if an agent selects bike mode for a trip, the travel time would be calculated by the Euclidian distance divided by a predefined bike speed, instead of calculating based on the shortest path in network. However, since MATSim is an open-source transportation simulation toolkit, it is possible to extend MATSim to incorporate bicycle traffic and bike-sharing.

Dubernet and Axhausen (2014) designed a prototypical simulation framework for a bike sharing system and incorporated with MATSim. They conducted a case study in Zurich and analyzed four scenarios with different bike re-distribution strategies, i.e. no redistribution vs optimal re-distribution. The simulation was running with 10% sample population for 200 iterations. Agents don't generate new plans for the last 10 iterations. The results indicate a significant difference in demand depending on the re-distribution strategy.

Ziemke et al. (2017) concentrated more on the bicycle traffic modeling in MATSim. The attributes of infrastructure were taken into consideration when simulating the decisions of cyclists. A more specific utility function was applied to cyclist in MATSim and a case study was conducted for the area near the campus of TU Berlin.

Hebenstreit and Fellendorf (2018) developed a dynamic bike-sharing module within a multimodal context. The module can simulate station-based bike-sharing and incorporate the interaction with other transport modes, like transit. The within day reschedule for bike-sharing trips is also supported by the module.

The extension of bike-sharing in MATSim is still under development and there is no module currently available. To simulate the bike-sharing system in the context of NYC, more efforts are needed to investigate the module development first.

## 6.5. Urban data observatory

NYU C2SMART has recognized the needs of a tool for sharing data and enhancing collaboration among researchers and practitioners, and developed a Common Innovation Platform (CIP). CIP provides an environment that allows two-way interaction with various communication and data tools by integrating four main components: A data storage system and analysis system, data repositories, project and task management tools, and a multifaceted collaborative project workspace. Each tool is combined through CIP using API capabilities into a single and easy navigable location.

For the MATSim project, we are encouraged to utilize CIP in order to share the back data (e.g. synthetic population) and results (e.g. aggregated mode share, simulated volumes). C2SMART Urban Data Observatory (UDO) is offering an interactive analysis and visualization of data, using PostgreSQL server. The data and its results after performing various analyses can be displayed to

all users in a collaborative workspace simultaneously, and authorized users are capable of performing operations on the UDO server. Accordingly, the MATSim project data (transit schedule and synthetic population) will be made accessible in UDO for authorized users and the analysis results will be displayed allowing custom querying in public. For instance, the query interface will provide several filters for users to select their interested synthetic population, including ages, work industries, trip purpose, origin/destination TAZs, etc. The users can also obtain some analysis results through the query interface, like the ridership of one transit line, the volume in peak hours for some major links, etc.

## Section 7: Technology Transfer, Dissemination, and Broader Impacts

### 7.1 Technology Transfer

We provide links to all the completed products we developed during this project as shown in Table 21. Each of the items in the table served on its own to transfer "new knowledge" or contributed to developing the product that did.

**Table 21. Delivered products**

| Output | Description |
|---|---|
| Synthetic population | Travel demand of NYC, including travel agendas, personal attributes and mode choices |
| Calibrated time-variant network | Time-variant multi-modal network for MATSim, with link free speed factors and capacity factors calibrated |
| SPSA calibration module | SPSA calibration module integrated with MATSim to calibrate link capacity factors |
| MATSim output analysis scripts | Transfer MATSim output from xml to csv and analyze mode share, travel time, etc. |
| Calibrated virtual test bed | MATSim baseline model for 2016 |
| Urban Data Observatory | Data sharing platform for C2SMART center |

### 7.2 Dissemination

The virtual test bed project was presented in a workshop2 hosted by the National Socio-Environmental Synthesis Center (SESYNC) of the University of Maryland in Annapolis, MD

---

2 The topic of the workshop is "SESYNC Pursuit: People, Land, Water And Fish: Integrating Social and Environmental Models in the Chesapeake Watershed". Organized by Center for Environmental Science, Horn Point Laboratory (UMCES), and the Center for Smart Growth Research and Education (NCSG) at the University of Maryland, funded by the National Science Foundation through the National Socio-Environmental Synthesis Center (SESYNC) of the University of Maryland as part of a research project.

(February 2019). The topic of the presentation is "Evaluating emerging transportation technologies and policies with a Network of Living Labs".

Another presentation was a guest talk by Brian He at ETH, Zurich (July 2019). The topic was "Evaluating emerging technologies and policies with a 'Network of Living Labs': Case of New York City".

A presentation was given by Dr. Chow to the International Chinese Transportation Professionals Association (ICTPA), US Northeast chapter, for their 25th Annual Meeting on October 5th, 2019. The topic was "A simulation-as-a-service ecosystem for evaluating mobility technologies and policies.

The work was presented by Brian He and Dr. Chow to local agencies and practitioners in a webinar "Open Source Multi-Agent Virtual Simulation Testbed – Applications for Congestion Pricing and COVID-19 Pandemic Recovery". The webinar link can be found here: https://www.youtube.com/watch?v=L4AMnFrz9kw.

Four papers were prepared directly as an output of the MATSim-NY tool. The first one "Evaluation of city-scale built environment policies in New York City with an emerging-mobility-accessible synthetic population" is under revision. Another paper "Calibration, validation, and application of multi-agent simulation test bed to New York City emerging transportation policies and technologies" is in preparation for submission to a journal. A third paper, "Traffic flow model calibration for an agent-based traffic simulation model applied in New York City", was accepted for presentation at DTA2020 (which was subsequently postponed due to COVID-19). A fourth paper on AV deployment optimization is being prepared entitled "Simulation-based optimization of autonomous taxi fleet service area design".

Several other papers were also prepared as part of the study of multimodal transport and emerging technologies for developing the tool during the study.

Papers:

- He, B. Y., Zhou, J., Ma, Z., Chow, J. Y. J., Ozbay, K., Evaluation of city-scale built environment policies in New York City using an emerging mobility-accessible synthetic population, working paper.
- He, B. Y., Zhou, J., Ma, Z., Wang, D., Sha, D., Lee, M., Chow, J. Y. J., Ozbay, K., Calibration, validation, and application of multi-agent simulation test bed to New York City emerging transportation policies and technologies, working paper.
- Wang, D., Ozbay, K., He, B.Y., Shen, B.Y., Chow, J.Y.J., 2020. Traffic flow model calibration for an agent-based traffic simulation model applied in New York City, Proc. DTA2020, Seattle, WA.
- Zhou, J., Chow, J.Y.J., Simulation-based optimization of autonomous taxi fleet service area design, working paper.
- Yoon, G., & Chow, J. Y. (2020). Unlimited-ride bike-share pass pricing revenue management for casual riders using only public data. *International Journal of Transportation Science and Technology*, 9(2), 159-169.
- Caros, N. S., & Chow, J. Y. (2020). Effects of violent crime and vehicular crashes on active mode choice decisions in New York City. *Travel Behaviour and Society*, 18, 37-45.
- Jung, J. Y., & Chow, J. (2019). Large-scale simulation-based evaluation of fleet repositioning strategies for dynamic rideshare in New York City (No. 2019-01-0924). SAE Technical Paper.
- Jung, J., & Chow, J. Y. (2019). Effects of charging infrastructure and non-electric taxi competition on electric taxi adoption incentives in new york city. *Transportation Research Record*, *2673*(4), 262-274.
- Allahviranloo, M., & Chow, J. Y. (2019). A fractionally owned autonomous vehicle fleet sizing problem with time slot demand substitution effects. *Transportation Research Part C: Emerging Technologies*, *98*, 37-53.
- Lee, M., Chow, J.Y.J., Yoon, G., He, B.Y., 2019. Forecasting e-scooter competition with direct and access trips by mode and distance in New York City, 99th Annual Meeting of the TRB, https://arxiv.org/abs/1908.08127.
- Rath, S., Chow, J. Y. J., 2019. Air Taxi Skyport Location Problem for Airport Access, https://arxiv.org/abs/1904.01497.
- Liu, Q., Chow, J.Y.J., A schedule-based dynamic transit passenger flow estimator using stop count data, working paper.

## 7.3 Broader Impacts

In addition to the direct dissemination and technology transfer, this research has led to a number of broader impacts.

The work has also been used in support of two other projects. The first is the C2SMART project on "Simulation and Analytical Evaluation of Bus Redesign Alternatives in Transit Deserts with Ride-hail Presence" by Dr. Chow in collaboration with Dr. Goldwyn at the Marron Institute. That study makes use of the MATSim-NYC model to evaluate bus networks in Brooklyn. A second project is the C2SMART study of NYC under COVID-19 ([http://c2smart.engineering.nyu.edu/covid-19-update-2](http://c2smart.engineering.nyu.edu/covid-19-update-2)) which uses MATSim-NYC to understand travel behavior pre- and post-COVID pandemic.

**Student training and involvement**: Several students have portions of their dissertations based on this project: Brian Yueshuai He, Jinkai Zhou, and Ding Wang. Through the Summer Undergraduate Research Program, several students have been trained as well: Matthew Shen, Carol Shlyakhova, and Ziyi Ma. Ziyi has gone on to work as a graduate researcher in support of this project and the bus redesign project while completing his MS degree. In addition to the main research team, we participated in the ARISE program to expose K-12 STEM students to this research and other projects from our lab. Material from this project have been included in Dr. Chow's graduate and undergraduate courses; for example, students make use of the OD demand queried from the synthetic population. This includes the use of the data for a Capstone project at CUSP working with startup company Dollaride from the Urban Future Labs.

The data has also supported the MS thesis topics for Mengyun Li (school student locations) and Yu Ching Emily Chao (parking activity in Manhattan).

**Public engagement**: The team presented our work at the NYU Tandon Research Expo[3], which exposes our project to the local community as well as to other students at NYU Tandon. The webinar "Open Source Multi-Agent Virtual Simulation Testbed – Applications for Congestion

---

[3] [https://engineering.nyu.edu/events/2019/05/03/2019-research-expo](https://engineering.nyu.edu/events/2019/05/03/2019-research-expo)

Pricing and COVID-19 Pandemic Recovery" has been made available to the public through Youtube.

**Industry engagement**: The team has presented the research to industry through the dissemination efforts mentioned above. In addition, the COVID impact study using MATSim-NYC has been presented to ITS-NY members as part of a Continuing Education program through Professional Development Hours. NYCDOT training workshops held each year include material from the MATSim-NYC model.

# References

511 Rideshare (2020). https://511nyrideshare.org/web/511ny-rideshare/trip-planner, last accessed June 5, 2020.

Abar, S., Theodoropoulos, G. K., Lemarinier, P., & O'Hare, G. M. P. (2017). Agent Based Modelling and Simulation tools: A review of the state-of-art software. Computer Science Review. https://doi.org/10.1016/j.cosrev.2017.03.001

Agarwal, A., Lämmel, G., & Nagel, K. (2018). Incorporating within link dynamics in an agent-based computationally faster and scalable queue model. Transportmetrica A: Transport Science, 14(5-6), 520-541.

Agarwal, A., Zilske, M., Rao, K. R., & Nagel, K. (2015). An elegant and computationally efficient approach for heterogeneous traffic modelling using agent based simulation. Procedia Computer Science, 52, 962-967.

Auld, J., Hope, M., Ley, H., Sokolov, V., Xu, B., & Zhang, K. (2016). POLARIS: Agent-based modeling framework development and implementation for integrated travel demand and network and operations simulations. *Transportation Research Part C: Emerging Technologies*, *64*, 101-116.

Aupperlee, A. (2017). Uber driver, self-driving software not at fault in Pittsburgh crash, company determines. Trib Live.

Balanced Transportation Analyzer. Retrieved from https://nurturenature.org/pages/balanced-transportation-analyzer.

Balmer, M., Rieser, M., Meister, K., Charypar, D., Lefebvre, N., & Nagel, K. (2009). MATSim-T: Architecture and Simulation Times. In Multi- Agent Systems for Traffic and Transportation Engenieering.

Balmer, M., Rieser, M., Meister, K., Charypar, D., Lefebvre, N., & Nagel, K. (2009). MATSim-T: Architecture and simulation. In A. L. C. Bazzan & F. Klugl (Eds.), Multi-agent systems for traffic and transportation engineering (pp. 57–78). Hershey, PA: IGI Global.

Becker, H., Balac, M., Ciari, F., & Axhausen, K. W. (2020). Assessing the welfare impacts of shared mobility and Mobility as a Service (MaaS). *Transportation Research Part A: Policy and Practice*, *131*, 228-243.

Bierlaire, M. (2018). PandasBiogeme: a short introduction. Technical report TRANSP-OR 181219. Transport and Mobility Laboratory, ENAC, EPFL.

Bonabeau, E. (2002). Agent-Based Modeling: Methods and Techniques for Simulating Human Systems. PNAS, Vol. 99, No. 3, 2002a.

BQX. (2018). BQX Completion of Conceptual Design Report. Retrieved August, 2019 from http://www.bqx.nyc/wp-content/uploads/2018/09/BQX_Completion_of_Conceptual_Design_Report_2018.08.pdf.

BQX. (2019). Retrieved August, 2019 from http://www.bqx.nyc.

Bradley, M., Bowman, J. L., & Griesenbeck, B. (2010). SACSIM: An applied activity-based model system with fine-level spatial and temporal resolution. Journal of Choice Modelling, 3(1), 5–31.

Brinckerhoff, P. (2014). 2010 Base Year Update and Validation of the NYMTC New York Best Practice Model. Retrieved from https://www.nymtc.org/LinkClick.aspx?fileticket=8WgNz6e-6dY=&portalid=0

Cetin, N., Burri, A., & Nagel, K. (2003). A parallel queue model approach to traffic microsimulations. Paper presented at the Transportation Research Board 82nd Annual Meeting, Washington, DC.

Chernick, M. R., & LaBudde, R. A. (2014). An introduction to bootstrap methods with applications to R. John Wiley & Sons.

Chow, J. Y. J. (2018). *Informed Urban Transport Systems: Classic and Emerging Mobility Methods toward Smart Cities*. Elsevier.

Chow, J. Y. J., & Djavadian, S. (2015). Activity-based market equilibrium for capacitated multimodal transport

systems. *Transportation Research Part C: Emerging Technologies*, *59*, 2-18.

Chow, J. Y. J., & Nurumbetova, A. E. (2015). A multi-day activity-based inventory routing model with space–time–needs constraints. *Transportmetrica A: Transport Science*, *11*(3), 243-269.

Chow, J. Y. J., & Recker, W. W. (2012). Inverse optimization with endogenous arrival time constraints to calibrate the household activity pattern problem. *Transportation Research Part B: Methodological*, *46*(3), 463-479.

Ciari, F., Balac, M., & Axhausen, K. W. (2016). Modeling carsharing with the agent-based simulation MATSim: State of the art, applications, and future developments. *Transportation Research Record*, *2564*(1), 14-20.

Cich, G., Knapen, L., Maciejewski, M., Bellemans, T., & Janssens, D. (2017). Modeling demand responsive transport using SARL and MATSim. *Procedia Computer Science*, *109*, 1074-1079.

Conway, M. W., Byrd, A., & van der Linden, M. (2017). Evidence-based transit and land use sketch planning using interactive accessibility methods on combined schedule and headway-based networks. Transportation Research Record, 2653, 45-53. https://doi.org/10.3141/2653-06

Conway, M. W., Byrd, A., & van Eggermond, M. (2018). Accounting for uncertainty and variation in accessibility metrics for public transport sketch planning. Journal of Transport and Land Use, 11(1). https://doi.org/10.5198/jtlu.2018.1074

Dennis, J. E., and D. J. Schnabel. (1989). A view of unconstrained optimization. Handbooks in Operation Research and Management Science (G.L. Nemhauser et al., Eds), Vol. 1, 1989, pp. 1-72.

Department of City Planning. (2015). NYC Open Data. Retrieved May 1, 2019, from https://data.cityofnewyork.us/Housing-Development/Public-Use-Microdata-Areas-PUMA-/cwiz-gcty

Dia, H. (2002). An Agent-Based Approach to Modeling Driver Route Choice Behavior Under the Influence of Real-Time Information. Transportation Research Part C, Vol. 10, 2002, pp. 331–349.

Djavadian, S., & Chow, J. Y. J. (2017a). Agent-based day-to-day adjustment process to evaluate dynamic flexible transport service policies. *Transportmetrica B: Transport Dynamics*, *5*(3), 281-306.

Djavadian, S., & Chow, J. Y. J. (2017b). An agent-based day-to-day adjustment process for modeling 'Mobility as a Service' with a two-sided flexible transport market. *Transportation research part B: methodological*, *104*, 36-57.

Dobler, C. and K. W. Axhausen (2011) Design and implementation of a parallel queue-based traffic flow simulation, Working Paper, 732, IVT, ETH Zurich, Zurich.

Dubernet, T. and K.W. Axhausen (2014) A multiagent simulation framework for evaluating bike redistribution systems in bike sharing schemes, Arbeitsberichte Raum- und Verkehrsplanung, 1010, IVT, ETH Zurich, Zurich.

Erath, A and Chakirov, A. 2016. Singapore. In: Horni, A, Nagel, K and Axhausen, K W. (eds.) The Multi-Agent Transport Simulation MATSim, Pp. 379–382. London: Ubiquity Press. DOI: http://dx.doi.org/ 10.5334/baw.57. License: CC-BY 4.0

Erdelić, T., Vrbančić, S., & Rošić, L. (2015). A model of speed profiles for urban road networks using g-means clustering. Paper presented at the 2015 38th International Convention on Information and Communication Technology, Electronics and Microelectronics (MIPRO).

GAO (2018). Public transit partnerships: Additional information needed to clarify data reporting and share best practices. GAO-18-539, U.S. Government Accountability Office.

Goulias, K. G., Bhat, C. R., Pendyala, R. M., Chen, Y., Paleti, R., Londuri, K. C., et al. (2011). Simulator of activities, greenhouse emissions, networks, and travel (SimAGENT) in southern California. Paper presented at the Transportation Research Board 91st Annual Meeting, Washington, DC.

Haglund, N., Mladenović, M. N., Kujala, R., Weckström, C., & Saramäki, J. (2019). Where did Kutsuplus drive us? Ex post evaluation of on-demand micro-transit pilot in the Helsinki capital region. *Research in Transportation Business & Management*, 100390.

Hebenstreit, C., & Fellendorf, M. (2018). A dynamic bike sharing module for agent-based transport simulation, within multimodal context. Procedia computer science, 130, 65-72.

Hidas, P. (2002). Modeling Lane Changing and Merging in Microscopic Traffic Simulation. Transportation Research Part C, Vol. 10, 2002, pp. 351–371.

Holland and Shah. (2019, December 4). Amazon, UPS and DHL are testing cargo bikes in New York City. Retrieved from https://www.cnbc.com/2019/12/04/amazon-ups-and-dhl-are-testing-cargo-bikes-in-new-york-city.html

Hörl, S., Ruch, C., Becker, F., Frazzoli, E., & Axhausen, K. W. (2019). Fleet operational policies for automated mobility: A simulation assessment for Zurich. Transportation Research Part C: Emerging Technologies. https://doi.org/10.1016/j.trc.2019.02.02

Horni, A and Nagel, K. 2016. More About Configuring MATSim. In: Horni, A, Nagel, K and Axhausen, K W. (eds.) The Multi-Agent Transport Simulation MATSim, Pp. 35–44. London: Ubiquity Press. DOI: http://dx.doi.org/10.5334/baw.4. License: CC-BY 4.0

Horni, A, Nagel, K and Axhausen, K W. (2016). Introducing MATSim. In: Horni, A, Nagel, K and Axhausen, K W. (eds.) The Multi-Agent Transport Simulation MATSim, Pp. 3–8. London: Ubiquity Press. DOI: http://dx.doi.org/10.5334/baw.1. License: CC-BY 4.0.

JSOM. (2018). Available at https://josm.openstreetmap.de.

Kang, J. E., Chow, J. Y. J., & Recker, W. W. (2013). On activity-based network design problems. *Transportation Research Part B: Methodological*, *57*(C), 398-418.

Konduri, K. C., You, D., Garikapati, V. M., & Pendyala, R. M. (2016). Enhanced synthetic population generator that accommodates control variables at multiple geographic resolutions. Transportation Research Record: Journal of the Transportation Research Board, (2563), 40-50.

Lam, T. C., & Small, K. A. (2001). The value of time and reliability: measurement from a value pricing experiment. Transportation Research Part E: Logistics and Transportation Review, 37(2-3), 231-251.

LIC Development MOU. Long Island City Development Project, Attachment A. https://d39w7f4ix9f5s9.cloudfront.net/4d/db/a54a9d6c4312bb171598d0b2134c/new-york-agreement.pdf. Accessed Nov 12.

Macal, C. M., & North, M. J. (2006b). Tutorial on agent-based modeling and simulation Part 2: How to model with agents. Proceedings of the 2006 Winter Simulation Conference, Monterey, CA.

Maciejewski, M., Bischoff, J., Hörl, S., & Nagel, K. (2017). Towards a testbed for dynamic vehicle routing algorithms. Communications in Computer and Information Science. https://doi.org/10.1007/978-3-319-60285-1_6

Major Citi Bike Expansion Map Revealed. Citi Bike. https://www.citibikenyc.com/blog/major-citi-bike-expansion-map-revealed. Accessed July 28,2019.

MARG (2016) PopGen: Synthetic Population Generator [online]. Mobility Analytics Research Group. Available at: http://www.mobilityanalytics.org/popgen.html, Accessed [September 2018].

Metropolitan Transportation Authority. (2018). Average Weekday Subway Ridership. Retrieved December 2019 from http://web.mta.info/nyct/facts/ridership/ridership_sub.html.

Nagel, K., Beckman, R. L., & Barrett, C. L. (1999). TRANSIMS for transportation planning. Paper presented at the 6th International Conference on Computers in Urban Planning and Urban Management, Franco Angeli, Milano, Italy.

Nagel, K, Kickhöfer, B, Horni, A and Charypar, D. 2016. A Closer Look at Scoring. In: Horni, A, Nagel, K and Axhausen, K W. (eds.) The Multi-Agent Transport Simulation MATSim, Pp. 23–34. London: Ubiquity Press. DOI: http://dx.doi.org/10.5334/baw.3. License: CC-BY 4.0

Nahmias-Biran, B.H., Oke, J.B., Kumar, N., Basak, K., Araldo, A., Seshadri, R., Akkinepally, A., Lima Azevedo, C. and Ben-Akiva, M., 2019. From Traditional to Automated Mobility on Demand: A Comprehensive Framework for

Modeling On-Demand Services in SimMobility. *Transportation Research Record*, p.0361198119853553.

NBC, 2019. Amazon opts out of building New York City headquarters. NBC News, https://www.nbcnews.com/tech/tech-news/amazon-opts-out-building-new-york-city-headquarters-n971636, February 14.

Neumann, A. 2016. Berlin I: BVG Scenario. In: Horni, A, Nagel, K and Axhausen, K W. (eds.) The Multi-Agent Transport Simulation MATSim, Pp. 369–370. London: Ubiquity Press. DOI: http://dx.doi.org/10.5334/ baw.53. License: CC-BY 4.0

New York Best Practice Model. Retrieved from https://www.nymtc.org/Data-and-Modeling/New-York-Best-Practice-Model-NYBPM.

New York City Department of Transportation. (2016). 2016 New York City Bridges Traffic Volumes. Retrieved December 2019 from http://www.nyc.gov/html/dot/downloads/pdf/nyc-bridge-traffic-report-2016.pdf.

New York City Department of Transportation. (2019). Traffic Volume Counts (2014-2018). Retrieved December 2019 from https://catalog.data.gov/dataset/traffic-volume-counts-2014-2018.

New York Metropolitan Transportation Council. 2040 SED Forecasts. New York, US. Transportation Information Gateway. Accessed on (September,8,2018) at https://tig.nymtc.org/views/24/table

New York Metropolitan Transportation Council. 2010/2011 Regional Household Travel Survey. New York, US. Transportation Information Gateway. Accessed on (June, 1, 2017) at https://www.nymtc.org/Portals/0/Pdf/SED/Excel.zip?ver=2016-05-26-130138-000

Pantelidis, T., Chow, J.Y.J., Rasulkhani, S., 2019. A path-based many-to-many assignment game to model Mobility-as-a-Service market networks, *arXiv preprint arXiv:1911.04435*.

Regional Plan Association. (2019). Congestion Pricing in NYC: Getting it right. Retrieved November, 2019 from https://www.rpa.org/publication/congestion-pricing-in-nyc-getting-it-right.

Rieser, M., Dobler, C., Dubernet, T., Grether, D., Horni, A., Lammel, G., Wariach, R., Zilske, M., Axhausen, K.W. & Nagel, K. (2014). MATSim user guide. Zurich: MATSim.

Rieser, M, Horni, A and Nagel, K. (2016). Scenarios Overview. In: Horni, A, Nagel, K and Axhausen, K W. (eds.) The Multi-Agent Transport Simulation MATSim, Pp. 367–368. London: Ubiquity Press. DOI: http://dx.doi.org/10.5334/baw.52. License: CC-BY 4.0.

Rieser-Schüssler, N, Bösch, P M, Horni, A and Balmer, M. 2016. Zürich. In: Horni, A, Nagel, K and Axhausen, K W. (eds.) The Multi-Agent Transport Simulation MATSim, Pp. 375–378. London: Ubiquity Press. DOI: http://dx.doi.org/10.5334/baw.56. License: CC-BY 4.0

Robbins, C. (Jan, 10th, 2020). De Blasio's Still Pushing The $2.7 Billion Streetcar Plan You Probably Forgot About. The Gothamist. Retrieved from https://gothamist.com/news/bqx-streetcar-nyc-to-shelbyville.

Robbins, H., & Monro, S. (1951). A stochastic approximation method. The annals of mathematical statistics, 400-407.

Rothfeld, R., Balac, M., Ploetner, K. O., & Antoniou, C. (2018). Agent-based simulation of urban air mobility. In *2018 Modeling and Simulation Technologies Conference* (p. 3891).

Shaheen, S., Cohen, A., & Jaffee, M. (2018). Innovative Mobility: Carsharing Outlook. UC Berkeley: Transportation Sustainability Research Center. http://dx.doi.org/10.7922/G2CC0XVW Retrieved from https://escholarship.org/uc/item/49j961wb

Small, K. (1982). The Scheduling of Consumer Activities: Work Trips. The American Economic Review, 72(3), 467-479. Retrieved June 2, 2020, from www.jstor.org/stable/1831545

Spall, J. C. (1988). A stochastic approximation algorithm for large-dimensional systems in the Kiefer-Wolfowitz setting. Presented at the 27th Conference on Decision and Control, Austin, Texas, USA, 1988.

Spall, J. C. (1998). An overview of the simultaneous perturbation method for efficient optimization. Johns Hopkins APL Technical Digest, Vol. 19, 1998b, pp. 482-492.

Spall, J. C. (1998). Implementation of the simultaneous perturbation algorithm for stochastic optimization. IEEE Transactions on Aerospace and Electronic Systems, Vol. 34, No. 3, 1998a, pp. 817-823.

U.S. Census Bureau; 2016 Census Summary File 1; Tables P1 and QT-P1; generated by John Smith; using American FactFinder; <http://factfinder.census.gov>; (12 August 2018).

U.S. Census Bureau. (2018). LEHD Origin-Destination Employment Statistics Data (2002-2015) [computer file]. Washington, DC: U.S. Census Bureau, Longitudinal-Employer Household Dynamics Program [distributor], accessed on {8 September 2018} at https://lehd.ces.census.gov/data/#lodes. LODES 7.3

Von Neumann, J. (1966). *Theory of Self-Reproducing Automata*. Edited by A. W. Burk. Urbana: University of Illinois Press.

Wong, Y. Z., Hensher, D. A., & Mulley, C. (2020). Mobility as a service (MaaS): Charting a future context. *Transportation Research Part A: Policy and Practice*, *131*, 5-19.

Yang, H. (1999). System optimum, stochastic user equilibrium, and optimal link tolls. Transportation Science. https://doi.org/10.1287/trsc.33.4.354

Yu, M., and W. D. Fan. (2017). Calibration of microscopic traffic simulation models using metaheuristic algorithms. International Journal of Transportation Science and Technology, Vol. 6, 2017, pp. 63-77.

Zhang, L. (2006). An Agent-Based Behavioral Model of Spatial Learning and Route Choice. Presented at 85th Annual Meeting of the Transportation Research Board, Washington, D.C., 2006.

Zheng, H., Son, Y. J., Chiu, Y. C., Head, L., Feng, Y., Xi, H., ... & Hickman, M. (2013). A primer for agent-based simulation and modeling in transportation applications (No. FHWA-HRT-13-054). United States. Federal Highway Administration.

Ziemke, D. 2016. Berlin II: CEMDAP-MATSim-Cadyts Scenario. In: Horni, A, Nagel, K and Axhausen, K W. (eds.) The Multi-Agent Transport Simulation MATSim, Pp. 371–372. London: Ubiquity Press. DOI: http://dx.doi.org/10.5334/baw.54. License: CC-BY 4.0

Ziemke, D., Metzler, S., & Nagel, K. (2017). Modeling bicycle traffic in an agent-based transport simulation. Procedia Computer Science, 109, 923-928.